THE JOURNAL OF BIOLOGICAL CHEMISTRY VOL. 289, NO. 32, pp. 22385–22400, August 8, 2014

Substitution of NS5 N-terminal Domain of Dengue Virus Type 2 RNA with Type 4 Domain Caused Impaired Replication and Emergence of Adaptive Mutants with Enhanced Fitness*

Received for publication, May 28, 2014 Published, JBC Papers in Press, June 5, 2014, DOI 10.1074/jbc.M114.584466

Tadahisa Teramoto[‡], Siwaporn Boonyasuppayakorn[‡], Misty Handley[‡], Kyung H. Choi[§], and Radhakrishnan Padmanabhan[‡1]

From the [‡]Department of Microbiology and Immunology, Georgetown University School of Medicine, Washington, D. C. 20057 and the [§]Department of Biochemistry and Molecular Biology, University of Texas Medical Branch, Galveston, Texas 77555-0156

Background: The four dengue virus serotypes, evolved from a common ancestor, are global human pathogens.
Results: Interserotypic substitution of the functional domain essential for 5′-capping was detrimental to RNA replication.
Conclusion: The chimeric RNA gradually evolves replication fitness through adaptive mutations in genes encoding two replication proteins.
Significance: This study provides a possible pathway for generating attenuated dengue virus vaccine.

Flavivirus NS3 and NS5 are required in viral replication and 5′-capping. NS3 has NS2B-dependent protease, RNA helicase, and 5′-RNA triphosphatase activities. NS5 has 5′-RNA methyltransferase (MT)/guanylyltransferase (GT) activities within the N-terminal 270 amino acids and the RNA-dependent RNA polymerase (POL) activity within amino acids 271–900. A chimeric NS5 containing the D4MT/D4GT and the D2POL domains in the context of wild-type (WT) D2 RNA was constructed. RNAs synthesized *in vitro* were transfected into baby hamster kidney cells. The viral replication was analyzed by an indirect immunofluorescence assay to monitor NS1 expression and by quantitative real-time PCR. WT D2 RNA-transfected cells were NS1- positive by day 5, whereas the chimeric RNA-transfected cells became NS1-positive ~30 days post-transfection in three independent experiments. Sequence analysis covering the entire genome revealed the appearance of a single K74I mutation within the D4MT domain ~16 days post-transfection in two experiments. In the third, D290N mutation in the conserved NS3 Walker B motif appeared ≥16 days post-transfection. A time course study of serial passages revealed that the 30-day supernatant had gradually evolved to gain replication fitness. Trans-complementation by co-expression of WT D2 NS5 accelerated viral replication of chimeric RNA without changing the K74I mutation. However, the MT and POL activities of NS5 WT D2 and the chimeric NS5 proteins with or without the K74I mutation are similar. Taken together, our results suggest that evolution of the functional interactions involving the chimeric NS5 protein encoded by the viral genome species is essential for gain of viral replication fitness.

Dengue viruses belong to the genus *Flavivirus*, within the family Flaviviridae. The genus *Flavivirus* contains at least 70 mosquito-borne or tick-borne viruses. Four serotypes of dengue virus (D1–D4[2]) are endemic or epidemic in >100 countries in tropical and subtropical regions of the world (1). Dengue viruses cause at least 100 million infections annually throughout the world. More recent estimates are ~3 times higher (2). Infected patients generally suffer from dengue fever, occasionally resulting in more severe diseases, especially during secondary infections by a different serotype, known as dengue hemorrhagic fever and/or shock syndrome with ~25,000 deaths each year (3).

The Dengue virus genomes are 5′-capped positive-sense single-stranded RNAs. The ~11-kb length genome encodes a single polyprotein, NH_2-C-prM-E-NS1-NS2A-NS2B-NS3-NS4A-NS4B-NS5-COOH, which is proteolytically cleaved by a combination of host- and virus-encoded proteases (NS2B-NS3) into three structural (C, prM, and E) and seven nonstructural (NS) proteins (NS1, NS2A, NS2B, NS3, NS4A, NS4B, and NS5). The NS proteins are responsible for directing viral RNA replication, including synthesis of negative and positive strand RNAs and the addition of 5′-cap to the positive sense RNAs.

NS5 plays important roles in these processes as a multifunctional protein. The N-terminal domain of NS5 possesses methyltransferase (MT) and guanylyltransferase (GT) activities necessary for forming a mature RNA cap structure that protects the viral genome and directs efficient translation (4–10). The first step in 5′-capping of the positive strand progeny viral RNA is hydrolysis of γ-phosphate of the 5′-triphosphorylated RNA, which is catalyzed by NS3 (11, 12). Then GT activity of NS5 adds a GMP, hydrolysis product of GTP, to the 5′-diphosphorylated RNA to yield GpppN-RNA (13). Finally, MT activity of NS5 transfers a methyl group from the *S*-adenosylmethionine (AdoMet) substrate to the N-7 position of the G in GpppN-RNA to yield $^{7\text{-Me}}$GpppN-RNA (cap 0 structure) (5) (for a

* This work was supported, in whole or in part, by National Institutes of Health Grant R01 AI087856 (to K. H. C and R. P).
[1] To whom correspondence should be addressed. Tel.: 202-687-2092; Fax: 202-687-1800; E-mail: rp55@georgetown.edu.

[2] The abbreviations used are: D1–D4, dengue virus types 1–4, respectively; D4MT/D2POL, chimera containing NS5 methyltransferase domain of D4 and the polymerase domain of D2; GT, guanylyltransferase; IFA, immunofluorescence assay; MT, 5′-RNA methyltransferase; NS, nonstructural protein; POL, RNA-dependent RNA polymerase; qPCR, quantitative real-time PCR; AdoMet, *S*-adenosylmethionine; aa, amino acid(s); nt, nucleotide(s).

review, see Ref. 14). The 5′-stem-loop structure of the viral RNA is critical for the *N*-7-methylation (5). A second methyl group is transferred to the 2′-OH moiety of the first nucleotide, A, of the viral RNA to yield $^{7\text{-Me}}\text{GpppA}_{2'\text{OMe}}$-RNA (cap1 structure) (4–10). Thus, 5′-capping of progeny viral RNA is processed through multiple enzymatic reactions. Little is known regarding the components of 5′-capping machinery, the RNA substrate requirements, and how these steps are modulated. For the dengue viruses, cap 1 structure is important for stability, efficient translation, and escape from the host innate immune response (reviewed in Refs. 14 and 15).

The C-terminal domain of flavivirus NS5 contains conserved motifs shared by all RNA-dependent RNA polymerases (POLs). NS5 was experimentally shown to have polymerase activity (16–18). In the cytoplasm of D2-infected cells, NS5 exists as a complex with NS3 (19) as well as other proteins required for viral replication and 5′-capping (20, 21). The nuclear localization signal in NS5, identified within the interdomain region between MT and POL domains, is also important for interaction with NS3, suggesting that NS3 binding masks the nuclear localization signal of NS5 and causes retention of the complex in the cytoplasm where the viral RNA replication occurs (for reviews, see Refs. 22 and 23 and references therein). Post-translational modification, such as phosphorylation, could expose the nuclear localization signal of NS5 and facilitate nuclear accumulation, albeit with unknown function.

NS3 is a multifunctional protein (22). The N-terminal region of NS3 is a NS2B-dependent serine protease (see Ref. 24 for a review and references therein). The C-terminal region is an ATP-dependent RNA helicase and has an ATP-independent RNA annealing activity (25). The ATPase active site of NS3 is also shared with that of 5′-RNA triphosphatase (11, 12). There is evidence for an interdomain interaction between the NS2B-tethered N-terminal NS3 protease domain and the C-terminal RNA helicase domain from the studies of NS3 mutations in the region downstream of the protease domain and upstream of the first conserved motif of RNA helicase domain of NS3 (26, 27). Thus, multiple activities of NS3 and NS5 function in two important processes in the virus life cycle, RNA replication and 5′-capping.

NS5 is a highly conserved viral protein. The amino acid sequence similarities of the overall viral polyproteins among the four Dengue virus serotypes (D1–D4) vary from 69% (D1 or D2 *versus* D4) to 78% (D1 *versus* D3). These amino acid sequence identities of NS5 protein *per se* from D1–D4 are slightly higher than those among the polyproteins of D1–D4 between 74% (D2 *versus* D4) and 82% (D1 *versus* D3). In this study, we sought to investigate whether the interaction between the two domains in NS5 plays a role in viral replication. The D2MT domain of NS5 was exchanged with that of D4 in the context of full-length D2 RNA because these two serotype sequences have the least sequence identity. Our results provide new insight regarding the coordinated function of NS3 and NS5 in the virus life cycle.

EXPERIMENTAL PROCEDURES

Construction of Plasmids—Construction of a full-length cDNA of D2 (New Guinea C strain) in yeast/*Escherichia coli* shuttle vector, pRS424, named pRS424FLD2, was described previously (28). In this study, we used the pRSR424FLD2-BcgI plasmid in which the BcgI site was engineered at the 3′-end of the D2 sequence. The BcgI restriction site was located 12 nucleotides downstream from the 3′ terminus of the cDNA encoding the D2 RNA in the plasmid. Digestion with BcgI would create a blunt end at the 3′ terminus of the cDNA, which upon *in vitro* transcription would generate an RNA as a run-off transcript without any additional nucleotides at the 3′-end (29).

Yeast homologous recombination (28–31) was used to generate full-length cDNAs containing chimeric NS5. Briefly, the full-length D2 cDNA, encoding the NS5 MT domain (corresponding to aa 1–270; nucleotide positions 7568–8377) that is targeted for substitution with the corresponding D4MT domain, was digested with restriction enzyme StuI (nucleotide positions 8960–8965; linear cDNA template 1). For the construction of the D2 cDNA containing the NS3 D290N mutation, the D2 cDNA was digested with XhoI (linear cDNA template 2). A PCR was performed to amplify the D4MT domain flanked by 33 nucleotides of D2 viral sequences both 5′ (in the NS4B region) and 3′ (in the POL domain) using the sense primer (5′-TCCATCATGAAGAACACAACCAACACGAGAAGGGGAACTGGGACCACAGGAGAG-3′) and the antisense primer (5′-TATTCTTTTCCCGATTATGTCTAGGTTTGGTATTTCTGTTTCAGTGGAGACACT-3′; PCR product 1). For construction of D4MT K74I/D2POL chimeric cDNA, the DNA fragment containing D4MT K74I was amplified by RT-PCR using the RNA extracted from the 30-day supernatant as the template and using the primers 7250F and 8600R (Table 1; PCR product 2). For the construction of D2 NS3 D290N mutant cDNA and the D4MT/D2POL cDNA containing the D2 NS3 D290N suppressor mutation, the DNA fragment containing the NS3 D290N mutation was amplified by RT-PCR using the RNA extracted from the 30-day supernatant as the template and the primers 5000F and 5700R (Table 1; PCR product 3). The PCR products were purified using a kit (Zymo Research). For the construction of NS5 D4MT/D2POL chimeric cDNA, the StuI-digested linear cDNA template 1 (see above) was mixed with the PCR product 1 prior to the yeast homologous recombination described below. For the construction of NS5 D4MT K74I/D2POL chimeric cDNA, the linear cDNA template 1 and the PCR product 2 were mixed prior to yeast homologous recombination. D2 containing the NS3 D290N mutation, the linear cDNA template 2 (see above) was mixed with PCR product 3 prior to yeast recombination. For the construction of D4MT/D2POL chimeric cDNA containing the NS3 D290N suppressor mutation, StuI-linearized D4MT/D2POL chimeric cDNA was mixed with PCR product 3 for homologous recombination. The competent *Saccharomyces cerevisiae* YPH857 cells were transformed with the corresponding cDNA and PCR product. After transformation, yeast harboring recombinant plasmids were selected on solid media lacking tryptophan. DNA was extracted from the positive yeast colonies and was used to transform *E. coli* Stbl2 (Invitrogen). The cDNA plasmid (pRS424-D2 encoding the D4MT domain) was isolated from transformed Stbl2 cells, and the DNA sequence of the chimeric NS5 was verified.

In Vitro Transcription, Electroporation, and Mammalian Cell Culture—Plasmid DNA was linearized at the 3′-end of the viral sequence with the restriction endonuclease BcgI and used as the template for *in vitro* transcription catalyzed by SP6 RNA polymerase (Epicenter Biotechnologies) in the presence of the $^{7\text{-Me}}$GpppG cap analog as described previously (32). RNA (~3 μg) was transfected by electroporation (Amaxa Nucleofector II system, Amaxa Biosystems, Cologne, Germany) into BHK-21 cells using the program A031. Briefly, ~1 × 10^6 cells were resuspended in 100 μl of Ingenio solution (Mirus Bio, Madison, WI). After pulsing, cells were carefully transferred into prewarmed complete medium (Dulbecco's modified Eagle's medium (DMEM), supplemented with 10% fetal bovine serum and 1× streptomycin/penicillin). Cells were allowed to recover for 5 min at 37 °C in an incubator. Cells were resuspended in 10 ml of complete DMEM and incubated in a T-12.5 flask. On days 2 and 9, cells were trypsinized and transferred into a T-25 and T-75 flask, respectively. This procedure was repeated using one-third of the trypsinized cells from a T-75 flask every 5–7 days.

Immunofluorescence—For IFA, RNA-transfected cells at the end of indicated time periods were seeded into a 1-cm^2 chamber slide (LabTek). Cells were fixed by treatment with acetone and were incubated with a 1:200 dilution of 7E11, a monoclonal antibody against D2 NS1 antigen. FITC goat anti-mouse immunoglobulin G conjugates (Kirkegaard & Perry Laboratories) were used as a secondary antibody at a 1:100 dilution. Immunofluorescence photomicrographs (×200 magnification) were acquired using a Leitz Diaplan microscope coupled to the Leica/Wild MPS48 automated photographic system. The numbers and intensities of positive cells were compared utilizing the ImageJ program (National Institutes of Health).

Viral RNA Extraction and Sequencing—After clarification of the culture medium at 13,000 rpm for 3 min at 4 °C, viral RNA was extracted from 500 μl of the supernatant using a mini-RNA kit (Qiagen). Cellular RNA was extracted with TRIzol® solution following the manufacturer's protocol (Invitrogen). Viral RNA was used as the template for reverse transcription in a 20-μl reaction volume containing 200 units of murine Maloney leukemia virus reverse transcriptase (New England Biolabs), the manufacturer-supplied buffer, random primers (3 μM), and dNTPs (500 μM). The entire region of NS5 was amplified with oligonucleotides corresponding to sense D2 nt 7251–7271 (NS4B) and antisense D2 nt 10,503–10,523 (3′-UTR). To sequence the entire genome to identify any compensatory mutations, ~1.2-kb-long overlapping fragments covering the viral genome were amplified with each specific primer pair (for the list of primers, see Table 1). The 5′ and 3′ termini of the genome were also sequenced by circularization of the RNA by ligation, followed by PCR (29).

Renilla Luciferase (Rluc) Reporter Replicon Assay—Construction of the D2 replicon encoding the *Rluc* reporter in pRS424 vector has been described previously (32). The BcgI site was created at the 3′ terminus of the replicon cDNA to generate *in vitro* RNA transcripts without extra non-viral sequences as described above. Then either the NS5 D4MT region or the NS3 D290N mutation was inserted into the WT D2 *Rluc* replicon cDNA using *in vivo* yeast recombination as described above for the construction of the full-length chimeric cDNA clones.

TABLE 1

Primers used for sequencing the cDNAs of chimeric viral RNAs

The cDNAs were amplified from chimeric viral RNAs with or without acquired mutations by RT-PCR as described under "Experimental Procedures."

Primer number[a]	Primer sequence
9F	TCT ACG TGG ACC GAC AAA GAC
222R	TCC TCG TCC CTG CAG CAT TCC
962F	AGA GAC TTT GTA GAA GGG GTT
1100R	AGT GGC AGG AGG TTG TTT GGC TTC
1767F	ACT GTT CAC AGG ACA TCT CAA
2300R	GAC TCC TAT GAG GAT TTT CAT
2970F	CAT GTC AGC GGC CAT AAA AGA
3260R	CAC CAC TGT GGT TCC TTC GCA
4000F	TGT CCG TTT CCC CAC TGT TCT
4200R	CAT TCT TTA GGA GTG AAC TGG
5000F	CAT ATG TGA GTG CTA TAG CCC
5200R	CGA CTC TAG TGG GGG CCA GGA
5700R	GGT TCT AGT CTT GAC ATA CTC
6000F	CTC CTA GAT AAC ATC AAC ACA
6200R	CAA AAC ACC ACC TTC TGT CTG
7000F	CTC AGT GAA CGT GTC CCT AAC
7250F	AAA CCC AAC TGT CGA TG
8200R(D4)[b]	GTT CCT GGA CAG CGG GCA TCT
8500F	AAC AAA CTG GAT CAG CAT C
8600R	TGT CAT TGC CAT CTG TGT CAC
9556F	CAA GAA TGG CCA TCA GTG GAG
9760R	GGT TTC TGC ATG GAA CTA CAA
10455F	TCT GGG AGG CCA CAA ACC ATG
10620F	CAG CAT ATT GAC GCT GGG AAA
3′endR	AGA ACC TGT TGA TTC AAC AGC

[a] F and R refer to forward and reverse primers. The primer numbers refer to their positions in the D2 genome of New Guinea C-strain (28).

[b] D4 primer is in the MT domain of NS5.

The replicon RNAs were made by SP6 polymerase-driven *in vitro* transcription in the presence of the $^{7\text{Me}}$GpppG cap analog. RNA (~3 μg) was electroporated into BHK-21 cells. In some experiments, in order to monitor the transfection efficiency, RNA transcribed *in vitro* from a plasmid encoding the firefly luciferase (*Fluc*) gene flanked by the 5′- and 3′-UTRs of the rabbit α-globin gene (pGLGpA; kind gift of Dr. Theo Dreher, Oregon State University) was mixed with *Rluc* replicon RNAs for transfection as follows. The pGLGpA plasmid encoding the *Fluc* gene was linearized by Acc65I, and the RNA transcript was made by *in vitro* SP6 RNA polymerase reaction (Ambion). 5′-capped *Fluc* RNA (0.1 μg) was mixed with replicon RNAs and electroporated into BHK-21 cells. Subsequently, cells were plated onto 6-well plates. The cells were periodically (3, 24, 48, and 72 h) lysed with 200 μl of 1× *Renilla* luciferase (*Rluc*) lysis buffer (Promega) or lysis buffer for the dual luciferase assay as recommended by the manufacturer (Promega). Aliquots (20 μl) of the lysates were used for measurement of *Fluc* and/or *Rluc* activity using a Centro LB 960 luminometer (Berthold Technologies) by injecting 50 μl of 1× *Rluc* or *Fluc* substrate with settings of 10-s reading and 2-s delay.

Quantitative Real-time PCR (qPCR)—D2 cDNA encoding the 5′-terminal 1–224 nt was made by PCR using the full-length D2 cDNA as the template. After purifying PCR products from agarose gel using a Zymogen kit, the DNA concentration was measured by absorbance ($A_{260\ nm}$) using a NanoDrop spectrophotometer ND-1000 (NanoDrop). This DNA was used as the standard for PCR to determine the copy number of the virus genome from the threshold cycle (C_t) value. Viral RNAs were extracted from supernatants using an RNA extraction kit (Qiagen) as well as from cells using TRIzol reagent (Invitrogen). The

cDNAs were generated from the extracted RNA using the murine Maloney leukemia virus reverse transcriptase reaction (20 μl) incubated at 42 °C for 2 h. Assuming 100% reaction efficiency, qPCR was performed in duplicate, including no-template controls that ensured a lack of signal in the assay background. Each cDNA solution was mixed with iQ^{TM}-SYBR Green supermix (Bio-Rad) and 12 pmol of primers in 20 μl of PCR mixture using the following conditions: initial denaturation at 95 °C for 30 s and then 40 cycles of 95 °C for 15 s, 55 °C for 30 s, and 72 °C for 30 s, using the iQ5 Multicolor Real-time PCR Detection System. The data were collected during each cycle at the 72 °C extension step with the iQ5 Optical System version 2.1 (Bio-Rad). The qPCR results were imported into Microsoft Excel, and the average values of duplicate C_t values were compared and converted to copy numbers of the viral genome. The amounts of intracellular viral genome were determined as ΔC_t values by comparing with cellular GAPDH RNA in the qPCR reaction using GAPDH-specific primers (32).

E. coli Expression of the NS5 D4MT/D2POL Protein and Purification—To express the chimeric NS5 protein, PCR was carried out using the primer 5′-TAAGGATCCGGAACTGGGACCACAGGAGAG-3′ containing the underlined BamHI site and the region between nt 7563 and 7583 from the D4 genome as the forward primer and the reverse primer, 5′-TAAAAGCTTCTACCACAGGACTCCTGCCTC-3′, containing the underlined HindIII site, nt 10,252–10,272, from the D2 genome and the template containing the full-length D2 cDNA encoding the NS5 D4MT domain. A 2.8-kilobase pair fragment was obtained. The PCR product was digested with BamHI and HindIII and cloned into pQE30 vector (Qiagen), also digested with the same restriction enzymes to yield the plasmid pQE30-NS5 D4MT/D2POL with an N-terminal His tag. The NS5 D4MT/D2POL encoding the K74I mutation (NS5 D4MT K74I/D2POL) in pQE30 vector was constructed from the cDNA obtained by RT-PCR of virion RNA extracted from the 30-day post-transfection supernatant using the same forward and reverse primers as above.

E. coli (XL1-Blue) cells were transformed with the plasmids and were grown in 1 liter of LB medium containing 100 μg/ml ampicillin and 0.5% glucose (w/v) at 37 °C. After $A_{600\,nm}$ reached 0.55–0.6, the bacteria were centrifuged at 5800 × *g* to remove any residual glucose and resuspended in 1 liter of LB medium containing 1 mM isopropyl-β-D-thiogalactopyranoside and 100 μg/ml ampicillin. The *E. coli* cells were incubated at 18 °C for 48 h and pelleted by centrifugation at 5800 × *g*. Cell pellet was resuspended using 30 ml of lysis buffer (100 mM Tris, pH 8.0, 300 mM NaCl, 20% glycerol, and 1× Complete^{TM} protease inhibitor mixture from Roche Applied Science). After three freeze in dry ice/thaw at room temperature cycles, the *E. coli* cell suspension was sonicated for 20 min at 40 watts (15 s on and 45 s off) on ice. After centrifugation of the cell lysate at 17,200 × *g*, the supernatant was mixed with 1.5 ml of Talon resin (Clontech) and incubated at 4 °C for 1 h. After washing the beads using the same lysis buffer four times and centrifugation at 800 × *g* for 1 min after each wash, the protein was eluted with 150 mM imidazole-containing buffer (100 mM Tris-HCl, pH 7.5, 300 mM NaCl, 20% glycerol) The eluate was dialyzed using a dialysis membrane (Spectra/Por®; M_r 1000 cut-off) against a buffer (100 mM Tris-HCl, pH 7.5, 300 mM NaCl, and 20% glycerol). The purified NS5 was stored in aliquots at −80 °C.

In Vitro POL Assay—POL activities of wild type and the chimeric NS5 were assayed using a minigenome RNA as the template (17, 29). The template RNA contained sequences from the 5′-end (224 nucleotides) fused to the 3′-end (493 nucleotides) of the D2 genome. PCR was performed using the forward primer that contained the modified T7-promoter sequence, which initiates transcription at A, the authentic D2 5′-end (5′-TAATACGACTCACTATTAG), and the reverse primer containing the 3′-terminal sequence (5′-AGAACCTGTTGATTCAACAG). After purification of the PCR product using a Zymogen kit, the RNA template was synthesized by T7-RNA polymerase (Epicenter Technologies). The transcribed RNA was quantified by spectrophotometry, and the integrity was verified by agarose gel electrophoresis.

The POL assay was performed in a standard reaction mixture (50 μl) containing 50 mM Tris-HCl (pH 8.0); 50 mM NaCl; 5 mM $MgCl_2$; template RNA (0.2 μg; 0.2 pmol); 500 μM each ATP, GTP, and UTP; 10 μM unlabeled CTP; and 10 μCi of [α-^{32}P]CTP along with 400 ng (4 pmol) of purified NS5. The reaction was carried out by incubation at 37 °C and at various time points was terminated by acid phenol-chloroform extraction, followed by purification with a Bio-Rad P-30 column to remove the unincorporated nucleotides. Radioactive RNA products were analyzed by formaldehyde-agarose gel electrophoresis and visualized by autoradiography (17). Band intensities were measured with ImageQuantTL software (GE Healthcare) in a PhosphorImager (Molecular Dynamics).

RNA MT Assay—The substrate RNA (200 nt from the 5′-end of the D2 RNA) for the MT assay was produced by *in vitro* transcription of the PCR fragment amplified from the pSY-2 plasmid (33). The standard PCR was performed using the forward primer that contained the T7 promoter (5′-CAGTAATACGACTCACTATTAGTTGTTAGTCTACGTG-3′) and the reverse primer (5′-AGTGAGAATCTCTTTGTCAGCTG-3′), pSY2 plasmid template, and AmpliTaq DNA polymerase (described in detail in Ref. 34).

The PCR-amplified DNA fragment was used as a template for *in vitro* transcription (34). RNA was recovered using the RNA Clean and Concentrator^{TM}-5 kit (Zymo Research). After checking the integrity of the RNA by gel electrophoresis, it was stored at −80 °C in aliquots.

A guanylyl cap was first added to the 200-nt RNA in a reaction (20 μl) containing 1 μg of RNA (4 μl), 10× ScriptCap m7G reaction buffer (500 mM Tris-HCl, pH 8.0, 60 mM KCl, and 12.5 mM $MgCl_2$) (2 μl), 10 mM GTP (2 μl), 10 μCi/μl [α-^{32}P]GTP (2 μl), 40 units/μl RNase inhibitor (0.5 μl), 10 units/μl vaccinia virus ScriptCap m7G capping enzyme (1 μl) and incubated for 1 h at 37 °C. After purification of the G-capped RNA, it was used as the template for MT activity of NS5. The components of the MT assay in a 10-μl volume were as follows: 1.5 μl of RNase-free water, 1 μl of 10× MT buffer (500 mM Tris-HCl, pH 7.5, 100 mM KCl, 20 mM $MgCl_2$, and 20 mM DTT), 0.5 μl of 8 mM AdoMet, 0.5 μl of 40 units/μl RNase inhibitor, 5 μl of 5′-cap-labeled RNA, and 1 μl of 10 μM D2 NS5 proteins. Following 1 h of incubation at 37 °C, the samples were passed through P-30 gel filtration columns (Bio-Rad), and RNAs were purified using the

kit. RNAs were treated with 1 unit of nuclease P1 in 0.75 M sodium acetate solution (1 μl for each reaction) and incubated for 1 h at 37 °C. The reactions were terminated by heating to 95 °C for 5 min, and the methylated and unmethylated species were separated by thin layer chromatography using 0.45 M ammonium sulfate as the solvent. α-^{32}P-Labeled species from the MT reaction were visualized and quantified using a PhosphorImager (Molecular Dynamics). Spot intensities were quantified using ImageJ (National Institutes of Health) and GraphPad Prism version 5.

RESULTS

Infectivity of Full-length D2 RNA Containing NS5 D4MT Domain Is Severely Impaired—In this study, we investigated the effect of substitution of the NS5 MT domain (aa 1–270) of D2 RNA with that of D4 on the ability to produce infectious virus. NS5 D4MT was chosen because sequence identity is the lowest between D2 and D4 among the four dengue virus serotypes, and they are evolutionarily distant from each other. The sequence identity between the D2MT and D4MT domains is 72.6% (Fig. 1*A*). Using homologous recombination in yeast, NS5 D2MT domain (4, 5) was replaced by the corresponding domain of D4.

Full-length wild type (WT) D2 RNA and D2 RNA encoding NS5 D4MT domain (hereafter referred as NS5 D4MT/D2POL chimera RNA) were generated by *in vitro* transcription and transfected into BHK-21 cells as described under "Experimental Procedures." An IFA specific for D2 NS1 was performed at various times post-transfection to monitor virus replication. WT D2 RNA-transfected cells produced virus, and most of the cells became NS1-positive by day 5, whereas NS5 D4MT/D2POL chimera RNA-transfected cells showed NS1 expression only after 15 days post-transfection and reached a level comparable with WT RNA at day 30 (Fig. 1*B*).

To measure the viral RNA levels, the viral RNAs were extracted from the supernatants containing the released virus particles. The intracellular viral RNAs were isolated from cells transfected with WT D2 RNA and the NS5 D4MT/D2POL chimera RNA. Samples were subjected to qPCR analysis as described under "Experimental Procedures." The viral RNA level from supernatant from WT D2 RNA-transfected cells had reached a plateau on day 5 (Fig. 1*C*). However, the viral RNA level from the NS5 D4MT/D2POL chimeric RNA-transfected cells reached this level on day 30 (Fig. 1*C*). We then measured the intracellular viral RNA levels for WT D2 RNA-transfected cells on day 5 and the NS5 D4MT/D2POL chimeric RNA-transfected cells on day 30 using the mRNA of the housekeeping gene, glyceraldehyde 3-phosphate dehydrogenase (GAPDH), as an internal control for normalization. The intracellular viral RNA copy numbers were similar for WT RNA-transfected cells on day 5 and the NS5 D4MT/D2POL chimeric RNA-transfected cells on day 30 (Fig. 1*D*). These results suggested that although the NS5 D4MT/D2POL chimeric RNA-transfected cells replicate more slowly than the WT D2 RNA-transfected cells, once enough viral proteins are translated and processed by cellular and viral proteases, viral RNA replication and virion assembly reach similar levels.

Sequence Analysis of the Recovered Viral RNAs Identified K74I in NS5 D4MT Domain or D290N in D2 NS3 Helicase Domain—To determine whether compensatory mutations have occurred, the released virus particles in the medium from the NS5 D4MT/D2POL chimeric RNA-transfected cells were collected periodically, and RNAs were extracted. The cDNAs produced by RT-PCR were sequenced as described under "Experimental Procedures." A single mutation at position 221 nt of the NS5 D4MT domain in the codon AAA to ATA, resulting in a $Lys^{74} \rightarrow$ Ile substitution, appeared 9 days post-transfection. In two of three independent experiments, the same K74I mutation occurred (Fig. 2*A*). The mutant virus quickly became the predominant species compared with the sequence of the original NS5 D4MT/D2POL chimera. WT D2MT domain has a Glu instead of Lys in the WT D4MT domain (*asterisk* in Fig. 2*C*).

In the third independent experiment, the NS5 D4MT/D2POL chimeric virus retained the original D4MT sequence even after day 65 post-transfection (Fig. 2*A*). Sequence analysis of the RNA showed the G868A mutation in the D2 NS3 gene on day 27 post-transfection (Fig. 2*B*). This mutation led to the D290N substitution in the Walker B motif in the NS3. The Asp at this location is conserved in other flaviviruses (Fig. 2*D*). Except for the ambiguity in reading the terminal ~20-nt regions in the 5′- and 3′-UTR, no other mutations were detected in all three experiments even at later time points beyond 60 days.

Our results suggested that the NS5 D4MT K74I or D2 NS3 D290N mutation conferred the NS5 D4MT/D2POL chimera virus selective fitness to recover from the debilitating substitution of the D4MT domain in the context of the D2 infectious clone. To confirm this acquired fitness of the chimera virus, we infected naive BHK-21 cells with supernatants of NS5 D4MT K74I/D2POL or NS3 D290N/D4MT/D2POL chimeric RNA-transfected cells collected at day 30 post-transfection, respectively, and monitored the infectivity by IFA. The chimeric virus with either of the acquired mutations, NS5 D4MT K74I or D2 NS3 D290N, replicated more slowly than the WT D2-infected cells at 3 days postinfection (Fig. 3, *A* and *B*). However, the time of appearance of NS1-positive cells in the chimeric NS5 D4MT K74I or D2 NS3 D290N virus-infected cells was faster than the original chimeric RNA because the NS1-positive cells appeared from day 2 postinfection (Fig. 3*C*). The extracellular viral RNAs extracted from the supernatants of the WT D2 and chimeric virus-infected cells were analyzed by qPCR (Fig. 3*D*). The results were consistent with the IFA data. Thus, these chimeric viruses replicated considerably faster than the time taken for the original NS5 D4MT/D2POL chimeric RNA to gain replication fitness in the transfected cells.

The Chimeric RNA Can Be Trans-complemented by Cotransfection of WT D2 NS5 Expression Plasmid—The virus replication of the NS5 chimeric RNA was slow, suggesting that either replication *per se* or assembly into infectious particles and cell-to-cell spread was inefficient compared with WT D2 RNA. We surmised that if the NS5 D4MT chimera in the context of full-length D2 RNA is defective due to incompatibility between chimeric NS5 and the reminder of the components of replication and/or 5′-capping complex, providing WT D2 NS5 in *trans* could at least partially restore the viral replication. We thus examined the effect of WT D2 NS5 cloned under the control of the pCMV promoter and supplied in *trans* by electroporation along with the full-length NS5 D4MT/D2POL chimera RNA

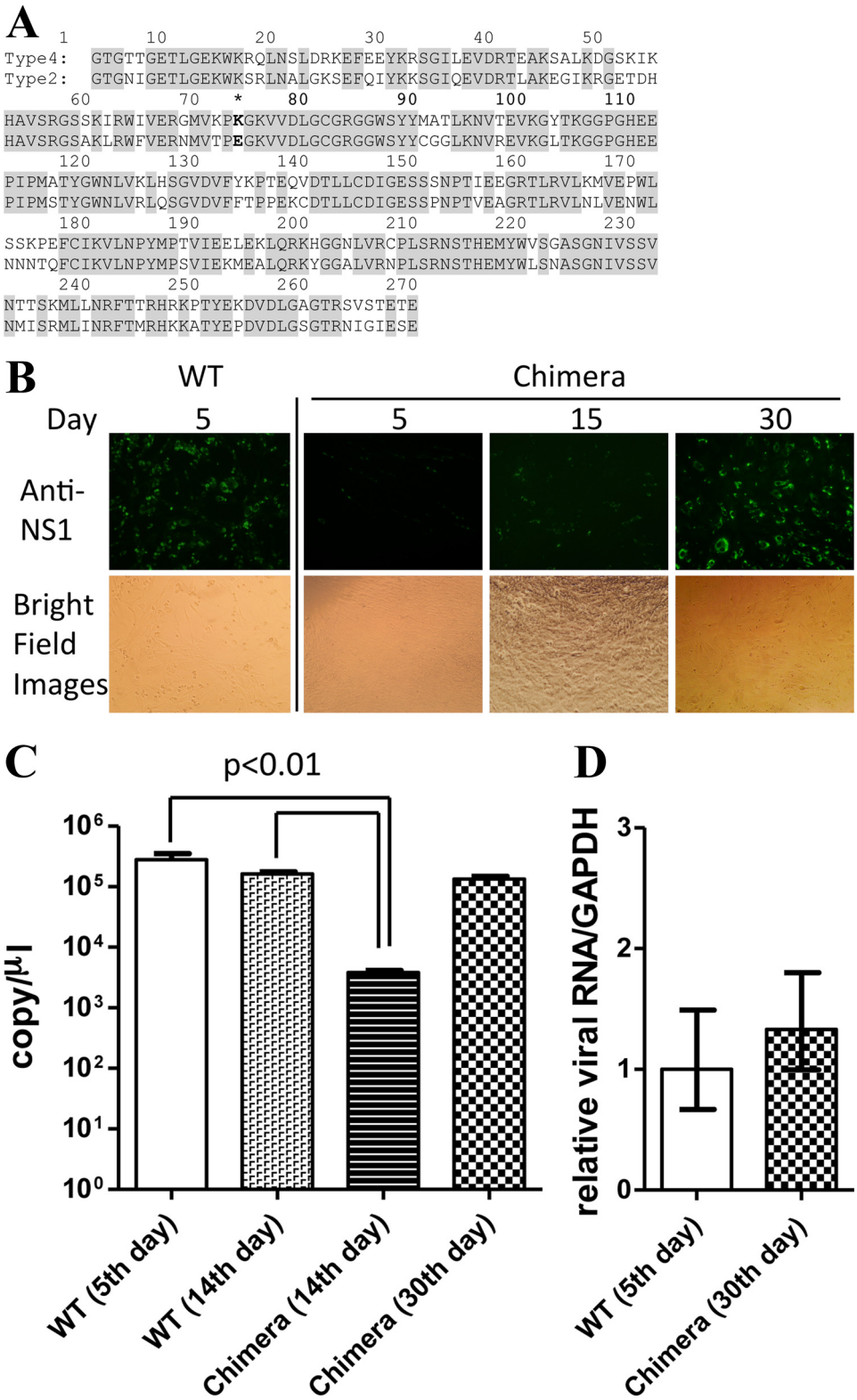

FIGURE 1. **The effect of substituting the NS5 MT domain of WT D2 with D4 analyzed by IFA and qPCR in BHK-21 cells.** *A*, alignment of the amino acid sequences of NS5 in the N-terminal regions, residues 1–270. The sequence identity between D4 and D2 in the MT domain is 72.6%. Identical amino acid residues are *shaded*. *B*, WT D2 RNA and NS5 D4MT/D2POL chimeric RNA were prepared by *in vitro* transcription in the presence of 5′-cap analog as described under "Experimental Procedures." The viral RNAs were transfected into BHK-21 cells, and at days 5, 15, and 30 post-transfection, cells were fixed, stained with an antibody specific for NS1, and analyzed by IFA. The conditions for IFA are described under "Experimental Procedures." *Top panels*, IFA of cultures at the indicated days post-transfection. *Bottom panels*, bright field images of cultures at the indicated days post-transfection. *C*, the viral RNAs were extracted from the supernatants from WT D2 RNA-transfected cells on days 5 and 14 and from NS5 D4MT/D2POL chimeric RNA-transfected cells on day 14 and 30 and were quantified by qPCR as described under "Experimental Procedures." $p < 0.01$. *D*, intracellular viral RNA levels of WT D2 at day 5 and NS5 D4MT/D2POL chimera at day 30 post-transfection were measured by qPCR. The viral RNA copy number values were normalized to GAPDH. *Error bars*, S.E.

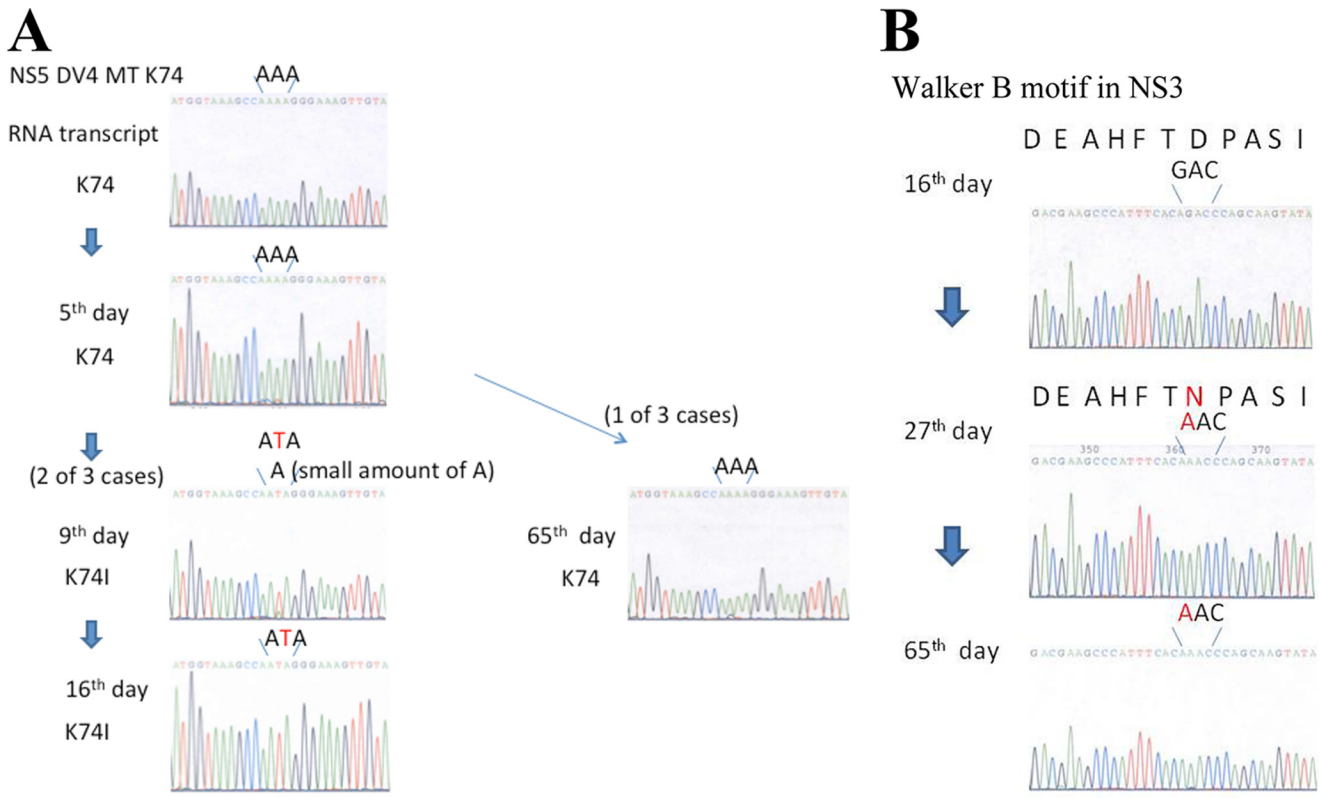

C

```
      53                    *                    112
D4:   …HAVSRGSSKIRWIVERGMVKPKGKVVDLGCGRGGWSYYMATLKNVTEVKGYTKGGPGHEE…
D2:   …HAVSRGSAKLRWFVERNMVTPEGKVVDLGCGRGGWSYYCGGLKNVREVKGLTKGGPGHEE…
D1:   …HAVSRGTAKLRWFVERNLVKPEGKVIDLGCGRGGWSYYCAGLKKVTEVKGYTKGGPGHEE…
D3:   …HAVSRGSAKLQWFVERNMVIPEGRVIDLGCGRGGWSYYCGGLKKVTEVRGYTKGGPGHEE…
WNV:  …HPVSRGTAKLRWLVERRFLEPVGKVIDLGCGRGGWCYYMATQKRVQEVRGYTKGGPGHEE…
JEV:  …HPVSRGSAKLRWLVEKGFVSPIGKVIDLGCGRGGWSYYAATLKKVQEVRGYTKGGAGHEE…
MVEV: …HPVSRGTAKLRWLVERRFVQPIGKVVDLGCGRGGWSYYAATMKRVQEVRGYTKGGPGHEE…
YFV:  …VAVSRGTAKLRWFHERGYVKLEGRVIDLGCGRGGWCYYAAAQKEVSGVKGFTLGRDGHEK…
TBEV: …LAVSRGTAKLAWLEERGYATLKGEVVDLGCGRGGWSYYAASRPAVMSVRAYTIGGKGHEA…
MEAV: …LSVSRGTAKLAWMEERGYVELTGRVVDLGCGRGGWSYYAASRPHVMDVRAYTLGVGGHEV…
```

D

```
      280          *
DENV    LIIMDEAHFTDPASIAARG
WNV     LFIMDEAHFTDPASIAARG
JEV     LFVMDEAHFTDPASIAARG
TBEV    VAIMDEAHWTDPASIAARG
HCV     IIICDECHSTDATSILGIG
```

FIGURE 2. **Sequence analysis of the RNA transcript before and after electroporation into BHK-21 cells on the indicated days.** *A*, the NS5 D4MT/D2POL chimeric RNA was synthesized by *in vitro* transcription and transfected into BHK-21 cells by electroporation as described under "Experimental Procedures." Sequence analysis of the region of interest in the vicinity of Lys^{74} in the D4MT domain is shown in the original RNA before electroporation and RNA isolated from supernatants (virions released into the medium) on days 5, 9, 16, and 65. In two of three independent experiments, Lys^{74} was mutated to Ile on day 9. In the third experiment, Lys^{74} was stable up to day 65 at this position. *B*, alignment of the amino acid sequences surrounding Lys^{74} (aa 53–112) in the N-terminal regions of different flavivirus NS5s. The adaptive mutation, K74I, in the NS5 D4MT/D2POL chimeric RNA was identified after serial passages in BHK-21 cells. The location of Lys^{74} is indicated in *boldface type* with an *asterisk* in *B*. *C*, in the third independent experiment, the Lys^{74} position was retained in NS5, but sequence analysis of the entire genome showed that the D290N mutation in D2 NS3 occurred on day 27, which was retained at least up to day 65. *D*, alignment of the amino acid sequences surrounding the Walker B motif of flavivirus NS3. The WT NS3 amino acid sequence from 280 to 298 is shown. The conserved Asp at position 290 indicated in *boldface type* with an *asterisk* is substituted by Asn in the NS5 D4MT/D2POL chimeric virus on day 27. *WNV*, West Nile virus; *JEV*, Japanese encephalitis virus; *MVEV*, Murray Valley encephalitis virus; *YFV*, yellow fever virus; *TBEV*, tick-borne encephalitis virus; *MEAV*, Meaban virus.

into BHK-21 cells. When NS5 D4MT/D2POL chimeric RNA and pCMV-NS5 expression plasmid (35) were cotransfected, multiple IFA-positive large clusters of cells appeared on day 9, and most of the cells became NS1-positive on day 15 (Fig. 4*A*). The viral RNA copy number was determined by qPCR. The result showed that the double transfection with the WT D2 NS5 expression plasmid produced 4 times higher RNA than the NS5 D4MT/D2POL chimeric RNA transfection alone (Fig. 4*B*). The sequence

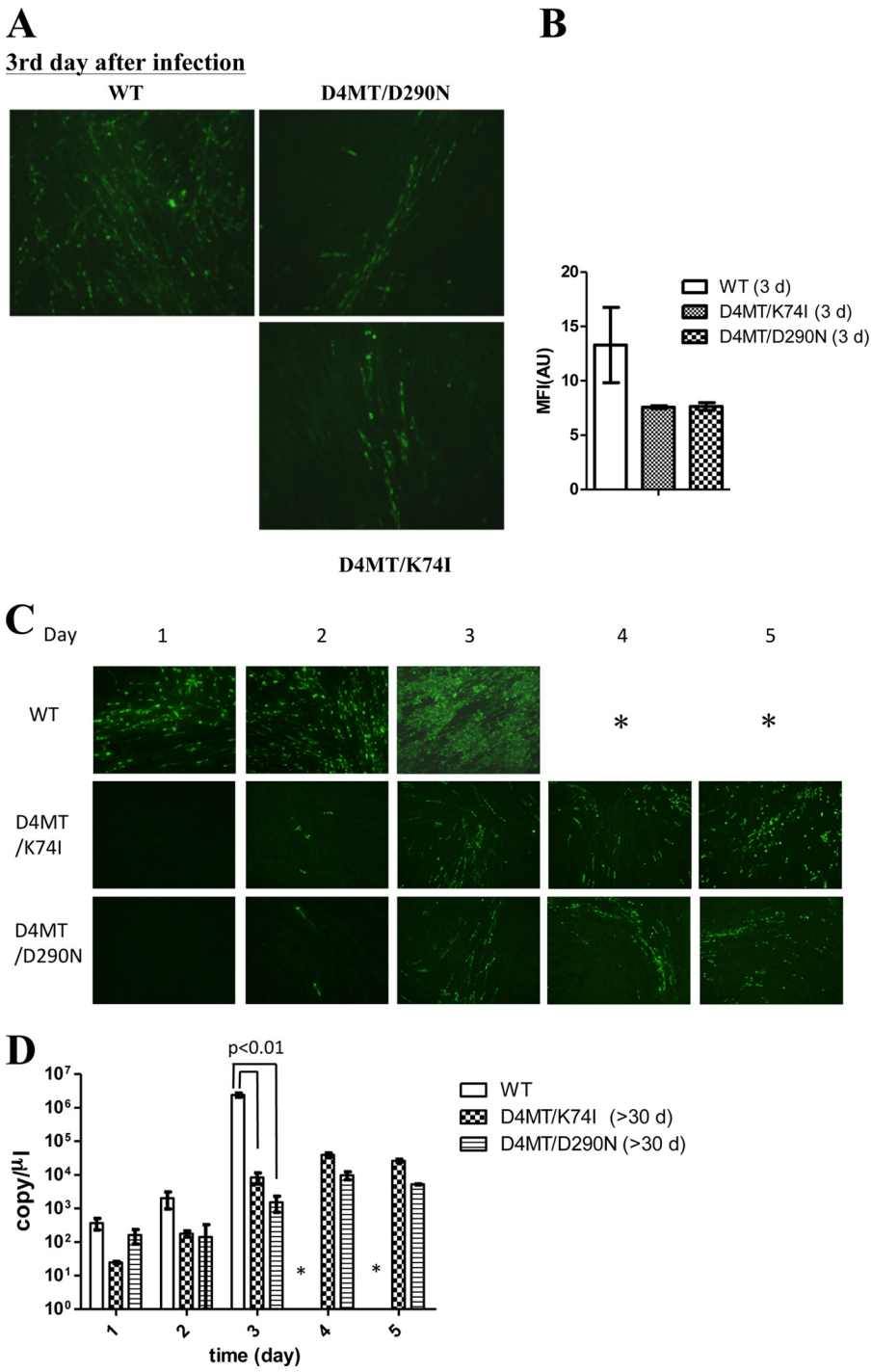

FIGURE 3. **IFA and qPCR of naive BHK-21 cells infected with supernatants from WT D2 or NS5 D4MT/D2POL chimeric RNA-transfected cells.** *A*, the supernatants from WT D2 or NS5 D4MT/D2POL chimeric RNA-transfected cells on day 5 or day 30 post-transfection, respectively, were incubated with naive BHK-21 cells. On the day 3 postinfection, RNA replication was monitored by IFA of NS1 protein expression. *B*, Mean fluorescence intensity (MFI) in arbitrary units (AU) as measured by NIH ImageJ of expression of NS1 in BHK-21 cells infected with 30-day supernatant containing chimera RNA harboring mutations. *C*, IFA of NS1 protein expression in the naive BHK-21 cells incubated for different time periods with supernatants from WT D2 or NS5 D4MT/D2POL chimeric RNA-transfected cells on day 5 or day 30 post-transfection, respectively. *, not done due to virus-mediated cytotoxicity. *D*, the viral RNAs were extracted from the supernatants from the naive BHK-21 cells incubated as described in *C* and were quantified by qPCR as described under "Experimental Procedures." $p < 0.01$. *, not done due to virus-mediated cytotoxicity. *Error bars*, S.E.

analysis of the RNA isolated from the virions released from the *trans*-complemented cells on day 9 revealed that the K74I mutation in the NS5 D4MT/D2POL chimeric RNA still appeared. These results suggest that there is a delay in viral replication of NS5 D4MT/D2POL chimeric RNA, which could be partially corrected by providing WT homologous D2 NS5 in *trans*.

Rluc Reporter Expression of WT and NS5 D4MT/D2POL Chimeric Replicon RNAs Reveals a Defect in Translation of the Newly Replicated Chimeric RNA—To test whether the decrease in viral RNA copy number in NS5 D4MT/D2POL chimeric RNA-transfected cells is due to the low translation efficiency or the slow replication rate of the viral RNA, we

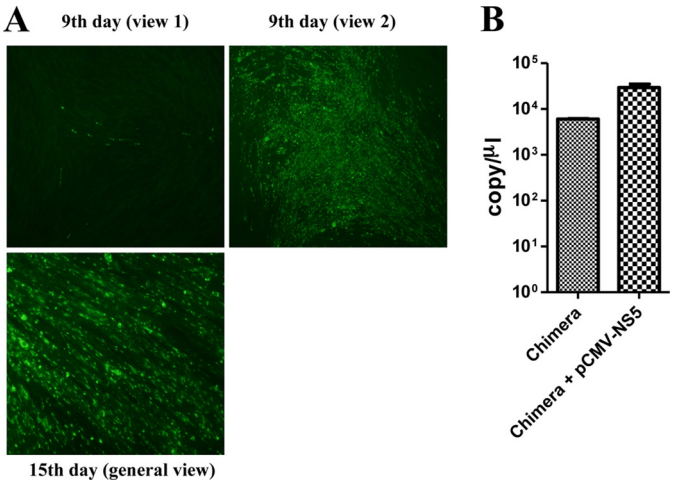

FIGURE 4. **Trans-complementation of WT D2 NS5 in replication-deficient NS5 D4MT/D2POL chimeric RNA-transfected BHK-21 cells.** *A*, NS5 D4MT/D2POL chimeric RNA and pCMV-D2 NS5 expression plasmid (35) were cotransfected into BHK-21 cells. Viral replication was evaluated by IFA of NS1 protein expression. *Top left*, the NS1-positive cells after 9 days post-transfection. There were clusters of NS1-positive cells seen on day 9 post-transfection (*top right*). On day 15, most of the monolayer cells were NS1-positive (*bottom*). *B*, NS5 chimera viral RNA levels were measured by qPCR on day 15. *Error bars*, S.E.

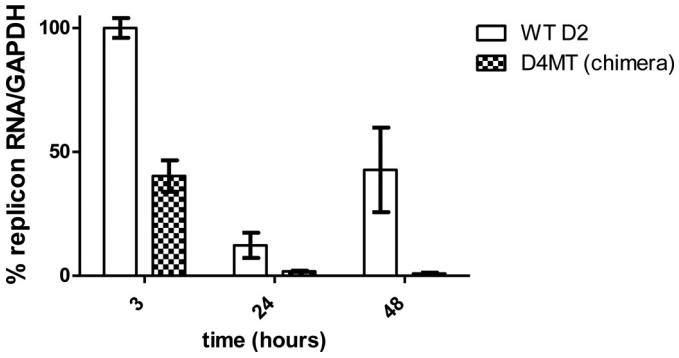

FIGURE 5. **Intracellular replicon RNA levels measured by qPCR.** The cellular RNAs were extracted from WT D2 or NS5 D4MT/D2POL chimeric RNA-transfected cells after 3, 24, and 48 h, and viral RNA levels were analyzed by qPCR as described under "Experimental Procedures." The viral RNA copy number values, calculated from C_t values, were normalized to GAPDH. *Error bars*, S.E.

sought to assess the efficiency of translation of WT D2 and NS5 D4MT/D2POL chimeric replicon RNAs. To this end, we constructed the NS5 D4MT/D2POL chimeric replicon RNA expressing *Rluc* reporter as well as the replicons containing the adaptive mutation K74I or D290N. The construction of WT D2 *Rluc* replicon RNA has been described previously (32). The 5′-capped *Rluc* reporter replicon RNAs were produced by *in vitro* transcription in the presence of 5′-cap analog. The 5′-capped NS5 D4MT/D2POL chimeric replicon RNA was translated with 2.5-fold less efficiency than the WT D2 replicon RNA, although translation efficiency of *in vitro* transcribed and 5′-capped *Rluc* replicon RNA is expected to be the same (Table 3). To examine whether this difference could be due to transfection efficiency, the levels of transfected viral RNAs in the same transfection experiment at 3 h post-transfection were measured by qPCR (Fig. 5). The input RNA level in the D4MT/D2POL chimeric RNA-transfected cells was 2.5-fold less abundant than WT D2 RNA (calculated from the C_t values; not shown), attributed to differences in the transfection efficiency of NS5 D4MT/D2POL chimeric RNA compared with WT D2 RNA. Based on this result, the translation efficiency of *in vitro*-capped WT and NS5 D4MT/D2POL RNA is the same (RLU 17,778 × 2.5 = 44,445). At 24 h post-transfection, the *Rluc* activities of both WT and the D4MT/D2POL RNAs decreased, probably due to decay of the *Rluc* protein, which has a half-life of ~3 h, as noted previously (32). During the 48 and 72 h post-transfection, in the WT D2 RNA-transfected cells, there was a dramatic increase in *Rluc* activity due to translation of newly replicated RNAs. In contrast, *Rluc* expression in cells transfected with the NS5 D4MT/D2POL chimeric replicon RNA remained low at 48 and 72 h (Table 3), indicating that translation of the newly replicated NS5 D4MT/D2POL chimeric replicon RNA is severely impaired (Table 3 and Fig. 5). In fact, the translation of the newly replicated NS5 D4MT/D2POL chimeric replicon RNA at the 72 h time point was ~300-fold lower than WT D2 replicon RNA (1,795,965/5955; see Table 3 and legend).

TABLE 2
***Fluc* activities in dual luciferase assays**

Sample[a]	3 h (*Fluc*)	Ratio (/WT)
No *Rluc* RNA	73,491 ± 1169	1.09 ± 0.01
WT D2 replicon RNA	68,379 ± 2471	1.00 ± 0.03
WT D2 RNA with D290N	63,893 ± 433	0.93 ± 0.006
NS5 D4MT/D2POL chimera RNA	47,463 ± 1872	0.69 ± 0.02
NS5 D4MT/D2POL RNA with NS3 D290N	61,227 ± 1602	0.89 ± 0.02
NS5 D4MT K74I/D2POL chimera RNA	50,843 ± 1265	0.74 ± 0.01
WT D2 noncapped RNA	88,973 ± 509	1.30 ± 0.007

[a] As an internal control, the GLGpA RNA (0.1 μg) was mixed with the respective *Rluc* replicon RNA (3 μg) and electroporated into BHK-21 cells, and dual luciferase assays were performed as described under "Experimental Procedures." The experiments were done in duplicate, and the *Rluc* activities were normalized (as given in Table 4) based on the *Fluc* activity shown here.

Next, we sought to examine the translation and replication of the NS5 D4MT K74I/D2POL and the NS5 D4MT/D2POL chimeric replicon RNA containing the NS3 D290N mutation because these mutations conferred replication fitness in the context of full-length chimeric RNA. The various 5′-capped *Rluc* replicon RNAs as well as the uncapped WT D2 replicon RNA as a control along with the GLGpA RNA encoding the *Fluc* gene as an internal control were transfected into BHK-21 cells. As a control, we also transfected 5′-capped WT D2 having a D290N mutation. *Rluc* (Table 4) and *Fluc* (Table 2) activities were measured by a dual luciferase assay as described under "Experimental Procedures." *Fluc* activities were used to normalize the *Rluc* activities. The *Rluc* activity of uncapped WT D2 replicon RNA was very low, close to the background level, due to low translation efficiency of the uncapped RNA compared with that of the *in vitro* capped replicon RNA (Table 4). On the other hand, the 5′-capped D2 WT having a D290N mutation showed *Rluc* activity ~20% less than the level obtained with the capped WT D2 RNA (Table 4).

Rluc expression in cells transfected with the NS5 D4MT/D2POL replicon RNA containing either K74I mutation in the D4MT domain or D290N mutation in the NS3 helicase domain showed a similar trend as the NS5 D4MT/D2POL chimeric replicon RNA and remained low at 48 and 72 h (Table 4). These results indicated that 5′-capping is important for viral RNA translation and hence replication. The *Rluc* expression with

TABLE 3

Translation and replication of WT D2 and NS5 D4MT/D2POL chimera *Rluc* replicon RNAs

	3 h	24 h	48 h	72 h
			RLU[a]	
No RNA	735 ± 159	825 ± 152	752 ± 163	801 ± 163
WT D2 replicon RNA[b]	42,983 ± 478	10,817 ± 222	562,288 ± 25,104	1,795,965 ± 143,724
NS5 D4MT/D2POL replicon RNA[b]	17,778 ± 263	894 ± 173	1345 ± 187	2382 ± 73

[a] Relative luciferase units; The *Rluc* values are expressed as mean with S.D. from duplicate wells.

[b] The level of NS5 D4MT/D2POL chimeric replicon RNA at the 3 h time point determined by qPCR was 2.5-fold less abundant than WT D2 replicon RNA due to differences in the transfection efficiency (Fig. 5) (C_t values not shown). Based on this result, the translation efficiency of *in vitro* capped WT D2 and NS5 D4MT/D2POL replicon RNAs is the same (RLU 17,778 × 2.5 = 44,445). The RLU at the 72 h time point is ~5955.

TABLE 4

Translation and replication of WT D2 and NS5 D4MT/D2POL chimera replicon RNAs

WT D2 *Rluc* replicon RNA and D2 replicon RNA encoding the D4MT/D2POL chimera with or without the K74I mutation in the D4MT/D2POL domain as well as with or without the D290N mutation within the D2 NS3 helicase domain were used in the experiments.

Sample	3 h	24 h	48 h	72 h
			RLU[a]	
No RNA	577 ± 16	591 ± 48	582 ± 22	575 ± 9
WT D2 RNA	33,345 ± 360	2,451 ± 38	33,941 ± 471	205,219 ± 839
WT D2 RNA with NS3 D290N mutation	25,257 ± 295	3,347 ± 37	51,722 ± 1574	163,326 ± 1980
NS5 D4MT/D2POL chimera RNA	43,422 ± 673	1512 ± 4	1009 ± 4	1135 ± 50
NS5 D4MT/D2POL chimera RNA with NS3 D290N mutation	48,292 ± 503	1060 ± 24	744 ± 4	724 ± 16
NS5 D4MT K74I/D2POL chimera RNA	37,600 ± 333	942 ± 42	857 ± 52	862 ± 29
WT-noncapped D2 replicon RNA	541 ± 35	496 ± 11	442 ± 5	762 ± 21

[a] The *Rluc* (RLU) values are expressed as mean with S.D. from duplicate wells. *Fluc* RNA was cotransfected as an internal control to monitor the transfection efficiencies as described under "Experimental Procedures." The RLU values were normalized in each case using the *Fluc* activities measured at 3 h time points from the cotransfection experiments of Fluc RNA. *Fluc* activities of samples are shown in Table 2.

WT and NS5 D4MT/D2POL replicon RNAs suggested that two factors could impact the *Rluc* activity: the translation efficiency, which is modulated by 5′-capping, and the replication efficiency. Both correlate with the available RNA template and viral replicase, which impact the viral RNA copy number in the transfected cells.

qPCR for Measuring the Replicon RNA Levels—We then tested whether the low *Rluc* activity in the NS5 D4MT/D2POL replicon RNA results from the low amount of replicon RNA. The viral RNA levels were measured by qPCR and normalized based on the cellular GAPDH RNA (Fig. 5). Interestingly, the difference in the levels of WT and NS5 D4MT/D2POL chimeric replicon RNAs at 48 h post-transfection was ~18-fold ($2^{5.5}$/2.5; calculated from C_t values; not shown), although the *Rluc* activity of WT D2 replicon RNA at 48 h was greater than ~167-fold of chimeric replicon RNA (Table 3). Thus, the NS5 D4MT/D2POL chimera replicon RNA was ~10-fold less efficient in translation compared with the WT D2 RNA (see "Discussion").

K74I Mutation in NS5 D4MT/D2POL Chimera or D290N Mutation in D2 NS3 Domain in the Context of Full-length RNA Restores Replication Fitness—The results in Tables 3 and 4 showed that the K74I mutation in the NS5 D4MT domain or the D290N mutation in D2 NS3 in the context of D4MT/D2POL replicon RNAs did not confer any selective fitness for replication within the 72-h incubation of replicon-transfected cells. Therefore, we sought to verify whether these adaptive mutations that emerged during the course of replication of full-length NS5 D4MT/D2POL chimera RNA could indeed confer replication fitness to full-length NS5 D4MT/D2POL chimera RNA. We engineered the K74I or D290N mutation individually into full-length NS5 D4MT/D2POL chimeric cDNAs, synthesized the respective RNAs by *in vitro* transcription, and transfected the RNAs into BHK-21 cells. The replication of the RNAs was analyzed by IFA for expression of NS1 as well as qPCR. The results shown in Fig. 6, *A* and *B*, indicate that these adaptive mutations in the context of full-length NS5 D4MT/D2POL chimeric RNAs enhanced translation of the viral protein as well as RNA replication in the 5′-capped RNA-transfected cells (Fig. 6, *A* and *B*). However, the 5-day supernatants from the transfected cells could not initiate a new round of translation and replication in naive BHK-21 cells in contrast to the ~30-day supernatants (see Fig. 3, *C* and *D*) (data not shown). These results suggested that the acquired mutations conferred a growth advantage to the D4MT/D2POL chimeric RNA. However, acquisition of adaptive mutations alone was not sufficient to produce infectious viral genome species released into the medium. Subsequent evolution of the viral genome species in the host cell environment during serial passages was required for assembly and release of infectious particles into the medium.

Polymerase and Methyltransferase Activities of Recombinant NS5 D4MT/D2POL Proteins Are Not Altered—Next, we sought to test the *in vitro* MT and POL activities of NS5 D4MT/D2POL with or without the K74I mutation. We expressed the chimeric NS5 proteins in *E. coli*. The purified full-length chimeric NS5 proteins (104 kDa) were used in our studies. POL activities of NS5 proteins were assayed using a D2 minigenome RNA as a template (17, 29, 33). The polymerase activities of the mutants and WT NS5s did not appreciably differ (Fig. 7, *A* and *B*). Under the reaction conditions used (37 °C), total RNA synthesis by elongation from the 3′-OH of the D2 minigenome RNA template was obtained, quantified, and plotted (Fig. 7, *A* and *B*) (17, 18).

Next, using the *in vitro* MT assays for both *N*-7- and 2′-*O*-methylations of guanylylated 200-nt 5′-D2 RNA substrate, we examined the MT activities of WT and NS5 D4MT/D2POL chimeric protein with or without the acquired mutation, K74I (Fig. 8 and Table 5). The MT activities of the recombinant WT or NS5 D4MT/D2POL chimeric proteins were also not significantly affected.

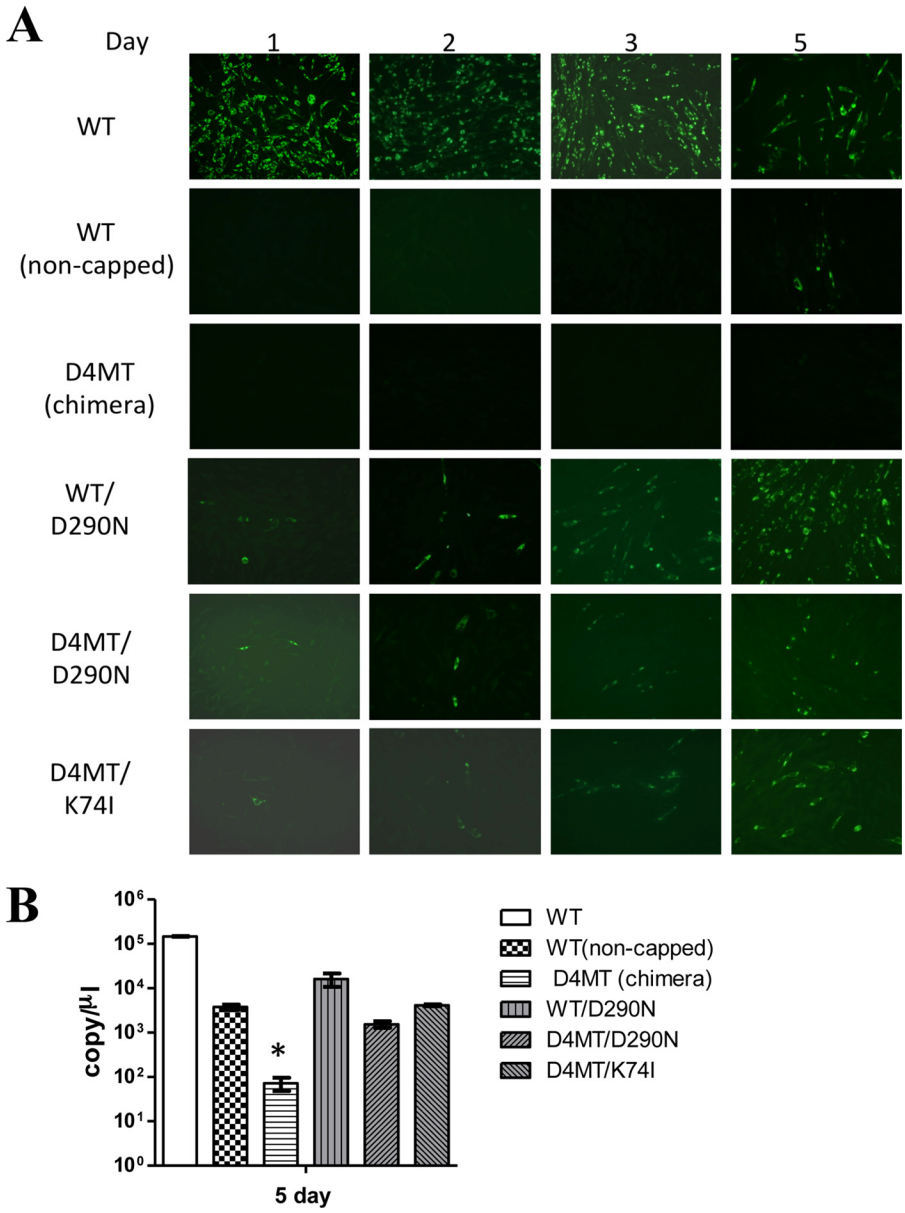

FIGURE 6. **IFA and qPCR of naive BHK-21 cells transfected with WT D2 or various mutant RNAs.** Shown are WT (capped or non-capped), D4MT chimera, WT-D290N, D4MT-D290N, and D4MT-K74I. *A*, each RNA transcript was transfected into BHK-21 cells, and at indicated days post-transfection, the viral protein NS-1 was visualized by IFA. *B*, viral RNA was purified from supernatants of transfected BHK-21 cells and quantified by qPCR. *Error bars*, S.E.

DISCUSSION

Flavivirus life cycle consists of multiple steps involving highly orchestrated protein-protein and protein-viral RNA interactions involving both viral and host proteins. These specific interactions could explain viral differences in pathogenicity that evolve over time and how viruses adapt to the distinct innate immune mechanisms mounted by both mammalian hosts and insect vectors to restrict their growth (for reviews, see Refs. 36 and 37 and the references therein).

Previous studies have shown that substitution of only the 3′-stem-loop structure of West Nile virus RNA with the corresponding region from D2 was detrimental for virus replication, albeit the two RNA elements are conserved in secondary structures analyzed by Mfold (38, 39). On the other hand, the substitution of 5′-UTR of West Nile virus RNA with that of D2 was somewhat tolerated (39). These results revealed that even when the viral proteins involved in RNA replication and assembly are derived from the same virus, their interactions with the critical RNA elements and the host proteins could be affected significantly by substitutions in the RNA template.

However, the region of flavivirus genome encoding the structural proteins can be largely replaced by the corresponding region from a heterologous flavivirus (40–42) or substituted by a unrelated reporter gene without affecting the replication of the viral RNA to any significant extent (43). The strategy of substitution of genes encoding structural proteins, prM and E, of different flaviviruses has been utilized to construct live attenuated chimeric viruses as vaccine candidates using the yellow fever virus or the attenuated D4 RNA as the backbone (40–42). However, point mutations or

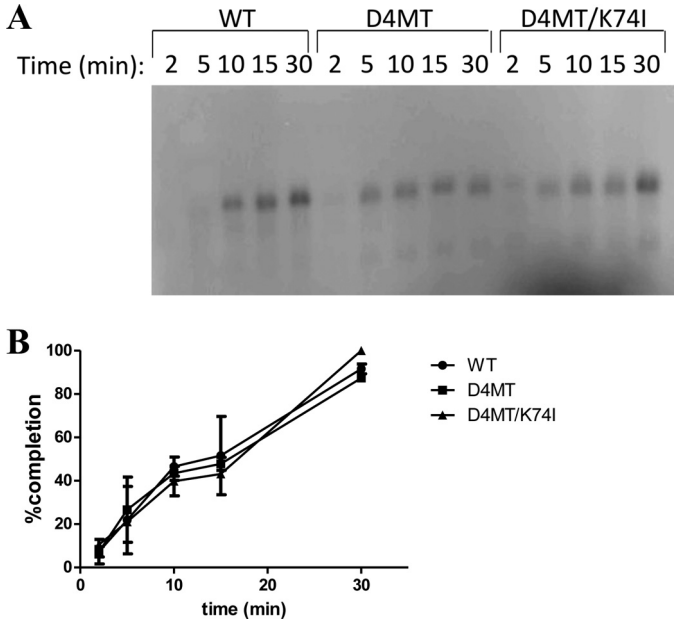

FIGURE 7. **Polymerase assays of WT D2 NS5, NS5 D4MT/D2POL, and NS5 D4MT K74I/D2POL proteins.** *A*, to evaluate the POL activity of recombinant NS5 proteins, the *in vitro* POL assay was performed using the D2 minigenome RNA as the template, D2 NS5, NS5 D4MT/D2POL, and the NS5 D4MT K74I/D2POL mutant, as described under "Experimental Procedures." *B*, the signal intensities of the labeled RNAs synthesized *in vitro* were quantified by the PhosphorImager and plotted. *Error bars*, S.E.

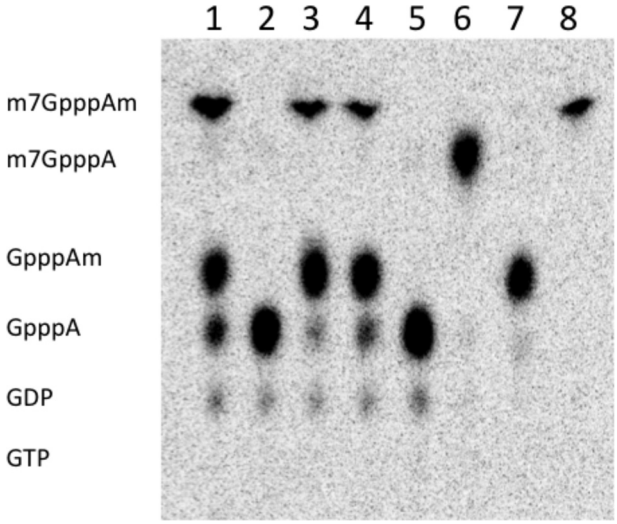

FIGURE 8. ***In vitro* 5′-RNA MT activity of WT D2 NS5, NS5 D4MT/D2POL, and NS5 D4MT K74I/D2POL proteins.** The 5′-labeled guanylylated capped RNA was incubated with 80 μM AdoMet and a 50 nM concentration of either D2 NS5 (*lane 1*), D2 NS5 POL domain (*lane 2*), NS5 D4MT/D2POL chimera (*lane 3*), or NS5 D4MT K74I/D2POL chimera (*lane 4*). The assay is described in detail under "Experimental Procedures." *Lanes 5–8*, TLC mobility markers for GpppA (*lane 5*), m7GpppA (*lane 6*), GpppAm (*lane 7*), and m7GpppAm (*lane 8*) species obtained using the vaccinia capping enzymes, where no enzyme (*lane 5*), ScriptCap™ m7G capping enzyme (*lane 6*), ScriptCap™ 2′-methyltransferase (*lane 7*), and ScriptCap™ m7G and 2′-*O*-methyltransferase capping enzymes (*lane 8*) were used. The radioactivity was quantified using a PhosphorImager and is shown in Table 5.

deletions of conserved motifs within the nonstructural proteins or *cis*-acting RNA elements were lethal due to their requirement for viral RNA replication (43, 44) (for reviews, see Refs. 22 and 23 and references therein).

TABLE 5

***In vitro* MT activities of recombinant WT D2 NS5 and NS5 D4MT/D2POL chimeric proteins**

The recombinant proteins are expressed in *E. coli* and purified as described under "Experimental Procedures."

Species	D2 NS5FL[a]	D2 NS5POL	D4MT/ D2POL	D4MT K74I/D2POL
	%	%	%	%
$^{7Me}GpppA_{2'\text{-}OMe}$	44.98 ± 0.79	0	44.76 ± 2.90	43.72 ± 6.45
$GpppA_{2'\text{-}OMe}$	43.22 ± 6.89	0	47.31 ± 2.03	46.04 ± 6.73
GpppA	11.80 ± 6.82	100 ± 0	7.92 ± 4.58	10.23 ± 5.91

[a] Values represent mean and S.E. of four values from two independent experiments (Fig. 8). The total radioactivity in each lane was normalized to 100%, and the percentage distribution of the radioactivity in various spots was calculated.

Viruses continuously evolve when subjected to intracellular or extracellular factors that restrict their genome replication. They gain replication fitness at least partially by acquisition of specific adaptive mutations, the rate of which is dependent on the extent of replicative block. For example, blocking the NS2B/NS3 protease-mediated internal cleavage of NS2A by substitution of lysine of the QKT → QST motif, did not impair viral replication but impacted virion assembly (45). Two types of suppressor mutations restored the function of the NS2A internal cleavage site; the first occurred by insertion of amino acid residues to restore cleavability at the NS2A site, and the second occurred by a suppressor mutation in the NS3 helicase domain, which revealed a functional link between NS2A and NS3 (45). In another study, a single conserved amino acid substitution, D146A in the MT domain of D1 NS5, abolished both *N*-7 and 2′-*O*-methylations of G-capped RNA and was lethal for viral replication (46). Continuous passage of culture supernatants from the D146A mutant RNA-transfected cells for infection of naive Vero cells for 12 days did not yield any plaques, indicating that the mutation was lethal for replication. However, transfection of the mutant RNA into BHK-21 cells stably expressing D1 replicon RNA was trans-complemented. Similarly, deletion of highly conserved NS5 POL motif, GDD → GVD, or the AdoMet binding site in the Kunjin virus NS5 MT domain (aa 78–87) could be trans-complemented by transfection of mutant genomic RNA into BHK-21 cells stably expressing Kunjin virus replicon (47). Dengue virus type 1 chimeras containing either West Nile virus MT or POL domain or complete NS5 was replication-defective but could be trans-complemented in D1 replicon-expressing cells (46).

In this study, we examined the effect of substitution of the entire MT domain of D2 NS5 (1–270 amino acid residues) with that of D4 in the full-length D2 RNA. The sequence identity between D2MT and D4MT domains is 72.6% (Fig. 1*A*). The N- and C-terminal domains of NS5 have distinct enzyme activities involved in 5′-capping and viral RNA replication. The C-terminal region of NS5 has POL activity that is required for viral replication (reviewed in Ref. 48). Moreover, the MT activity of full-length NS5 in the synthesis of fully methylated product, $^{7Me}GpppA_{2'\text{-}OMe}$, was 2-fold higher than the N-terminal domain alone (data not shown), suggesting that the conformation of full-length NS5 and/or an interdomain interaction between the N- and C-terminal regions of NS5 facilitates the MT activity. Therefore, we hypothesized that substitution of an entire functional domain of D2 serotype with that of D4 could interfere with one or both functions of NS5 if precise molecular

interactions among homologous viral components are required in 5′-capping and RNA replication. In this study, we show for the first time that the two functional MT domains involved in 5′-capping could be interchanged between two evolutionarily distant dengue virus serotypes, D2 and D4. Although the viral replication was initially severely impaired, by repeated passages of BHK-21 cells transfected with mutant chimera RNA, an attenuated chimera virus evolved with enhanced viral replication fitness with a single amino acid change, K74I, in the MT domain of chimeric NS5 or highly conserved D290N in the NS3 helicase domain.

In a previous study (49), mutagenesis of 17 amino acid residues of the D2MT domain that were predicted to be involved in *S*-adenosylmethionine binding (Ser^{56}, Trp^{87}, and Asp^{131}) and/or MT enzyme catalysis (S56A, W87I, W87K, and D131A) drastically affected MT activity. Moreover, the clustered mutations targeting the *S*-adenosylmethionine binding pocket (K76A/D79A and G81A/G83A/G85A) or the mutation of MT active site residues (D146A/E149A) all either abolished or severely reduced both N-7 and 2′-OMe activities (>90%). Interestingly, the S46A and D131A mutations were unstable and reverted back to WT (49). The sequence alignment of the D2MT domain that was substituted with D4MT (Fig. 1*A*) shows that all of these amino acid residues that were shown to be important for N-7 and 2′-OMe activities and viral replication (49) are conserved in the D2MT and D4MT domains. This observation may explain why the MT activities were not affected (Fig. 8 and Table 5) by the D2MT substitution with D4MT.

We have shown in this study that the *in vitro* MT and POL enzyme activities of WT D2 NS5 and the mutant NS5 chimeric proteins are not significantly different. The POL activity assay was performed at 37 °C under conditions that favored total RNA synthesis by elongation of self-primed minigenome RNA template (17, 18). Therefore, the existence of subtle differences in enzyme activities of WT D2 NS5 POL and the two mutant chimeric NS5 proteins in *de novo* initiation cannot be ruled out.

The rate of replication of the full-length RNAs was considerably delayed. This observation suggests that the amino acid residues that are different in the D4MT domain compared with D2MT are contributing to this replication block in the chimera viral RNA. Moreover, we passaged the NS5 D4MT/D2POL chimeric RNA-transfected cells for 30 days, rather than the supernatants from the transfected cells, which resulted in stable attenuated chimeric viruses with adaptive mutations in three independent experiments. In two experiments, the same K74I within the D4MT domain in the chimera virus first appeared on day 9. In the third, D290N mutation in the D2 NS3 Walker B motif was observed after day 16 and was stable even up to day 65. Interestingly, the K74I mutation occurred earlier than the D290N mutation. We further confirmed that the virus encoding the NS5 D4MT chimeric RNA with the acquired K74I mutation indeed replicated faster in BHK-21 cells than in the original NS5 D4MT/D2POL RNA-transfected cells before acquiring the mutation (Figs. 3 and 6 *versus* Fig. 1).

It is interesting that the NS5 D4MT/D2POL RNA acquires the K74I mutation instead of the Glu that is conserved in the D1, -2, and -3 MT domains. However, Japanese encephalitis virus and Murray Valley encephalitis virus MT domains have Ile at this position (Fig. 2*C*). Lys^{74} is located on the surface of the MT domain, away from the MT active site (Fig. 9*A*). In the crystal structure of Japanese encephalitis virus NS5, Lys^{74} in MT is located near the POL domain, although it is not in the interface (50) (Fig. 9*B*). Thus, it is possible that Lys^{74} is important for protein-protein interaction, such as with NS3 required for coordination of RNA synthesis and capping.

The second acquired mutation was D290N in NS3. Asp^{290} is highly conserved in the *Flaviviridae* family, including dengue virus, West Nile virus, Japanese encephalitis virus, tick-borne encephalitis, and hepatitis C virus (12), and is a part of the Walker B motif in the NS3 helicase domain (Figs. 2*C* and 9*A*, *right*). Asp^{290} is also exposed to solvent and thus could potentially be involved in the NS3 and NS5 interaction. NS3 and NS5 are shown to interact in D2-infected cells (19, 51). Using a yeast two-hybrid assay, the C-terminal region encompassing amino acid residues 303–618 of NS3 was shown to interact with the interdomain linker region of NS5 spanning residues 320–368 (52). Lys^{330} of NS5 was shown to be important for interaction with NS3 (53). However, in another study using an AlphaScreen assay based on chemiluminescence signal released by two interacting proteins, it was shown that the interaction of the N-terminal NS3 protease domain with full-length NS5 was stronger than the NS3 helicase domain alone but still less than with the full-length NS3 (54). Perhaps this acquired mutation in D2 NS3, D290N, compensates for the unfavorable molecular interactions between WT D2 NS3 and NS5 D4MT/D2POL chimera during viral RNA replication and/or 5′-capping.

Using *Rluc* reporter replicon RNAs, we provide evidence that the replication defect in RNA encoding the NS5 D4MT/D2POL is probably due to a defect in translation of newly replicated RNA. Translation of the newly replicated replicon RNAs encoding the NS5 D4MT/D2POL was dramatically decreased between 48 and 72 h post-transfection (Tables 3 and 4). The qPCR analysis showed that intracellular RNA levels for WT replicon RNA are only ~18-fold higher at 48 h than the NS5 D4MT chimeric RNA, whereas the *Rluc* activities (translation) for WT replicon are ~167-fold at 48 h and ~300-fold at 72 h higher than the replicon encoding NS5 D4MT/D2POL chimera (Tables 3 and 4). This discrepancy again suggests that the newly replicated template RNAs in chimera RNA-transfected cells are defective in translation, probably due to 5′-capping deficiency based on our results of *Rluc* activities of uncapped replicon RNA. Inefficient translation would lead to reduced accumulation of sufficient viral replicase complex required for amplification of viral templates.

When the compensatory mutation, K74I, was introduced into the replicon RNA encoding the NS5 D4MT/D2POL chimera, it did not enhance the replication fitness of NS5 D4MT/D2POL replicon RNA within the incubation period of 72 h. To explain this unexpected result, we surmised that infectious virions produced from full-length RNA encoding NS5 D4MT/D2POL chimera were evolved during continuous passaging for 30 days to gain replication fitness. The viral RNA genome species containing the acquired mutation (NS5 D4MT K74I or NS3 D290N) in the 30-day supernatants were capable of initi-

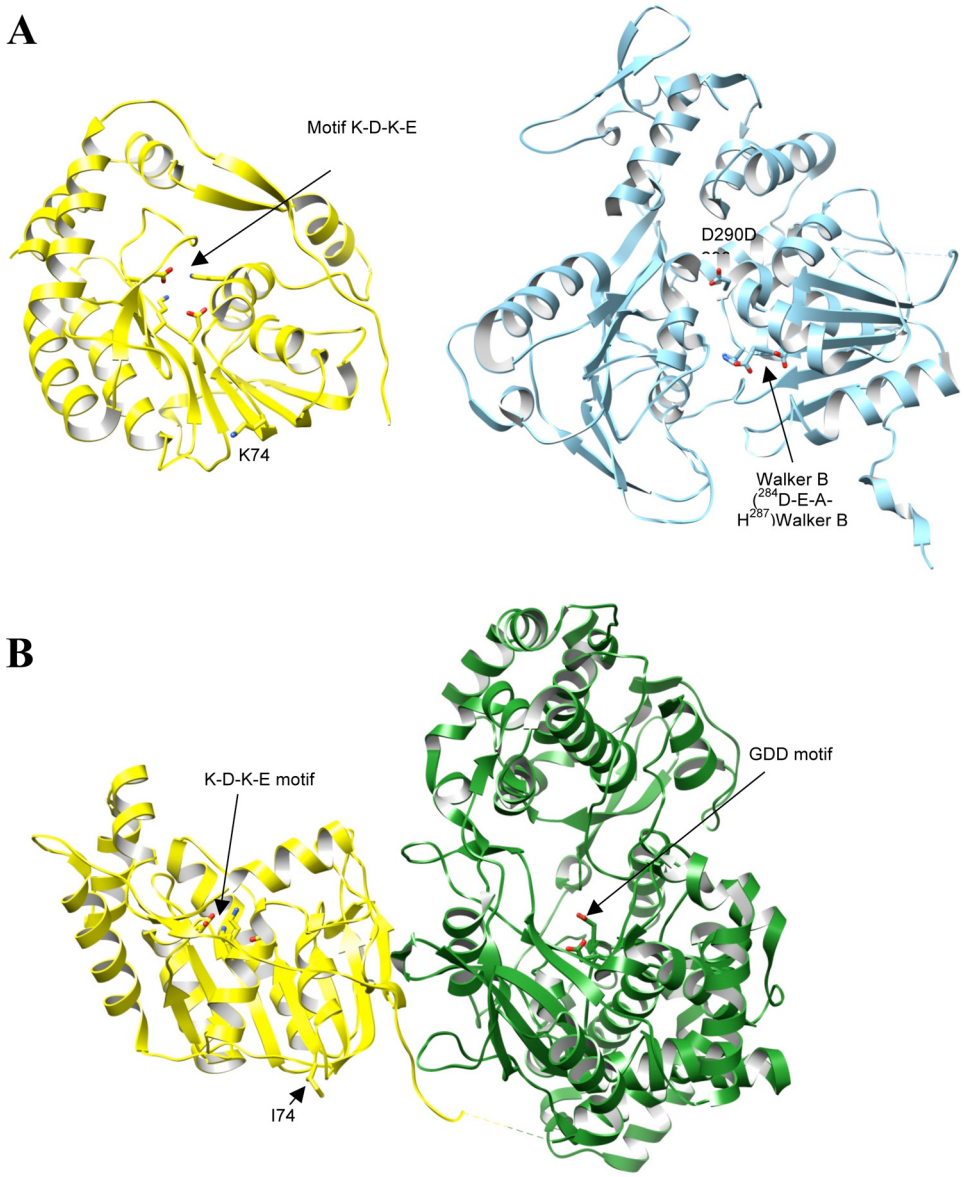

FIGURE 9. **Locations of Lys^{74} and Asp^{290} mutations in the structures of NS5 and NS3 helicase.** *A*, structures of D2MT (Protein Data Bank accession code 2P41) and NS3 helicase domain (Protein Data Bank accession code 2BMF). MT active site residues (Lys^{61}, Asp^{146}, Lys^{182}, and Glu^{218} motif) and Lys^{74} are depicted in *stick models* for reference (*left*). The Walker B motif (Asp^{294}, Glu^{295}, Ala^{296}, and His^{297}; Fig. 2*D*) in NS3 helicase and Asp^{290} are shown in *stick models* (*right*). *B*, Japanese encephalitis virus NS5 (Protein Data Bank accession code 4K6M) that has Ile^{74} in the MT domain. The MT and POL domains are shown in *yellow* and *green*, respectively.

ating infection in naive BHK-21 cells (Fig. 3). However, the supernatants from a 5-day incubation of RNAs containing the adaptive mutations were inactive in this regard. We believe that the quasispecies that accumulate in the 30-day period give enhanced fitness for the chimeric virus. The RNA viruses that depend on error-prone RNA-dependent RNA polymerase for their replication are endowed with the ability to generate quasispecies, which give them the power to adapt to new environmental insults and challenges, as described previously for poliovirus (55).

In contrast, we surmise that the K74I mutation introduced into the D2 replicon RNA encoding the NS5 D4MT K74I/D2POL chimera was not subjected to selective pressure for replication of the replicon RNA. It is possible that replicon RNA is less capable of generating quasispecies due to conformational changes in the RNA as a result of an insertion of a reporter gene and/or lack of cell-to-cell spread, time of incubation, and imposed selection pressure for replication. Future experiments are likely to reveal the specific step that is defective for replication in the chimeric virus that is compensated in the 30-day supernatant. Further work is necessary to understand the specific molecular interactions among the components of flaviviral replication and 5′-capping complexes that are involved in the dengue virus life cycle.

Acknowledgment—We acknowledge the contribution of Dr. Mini Kapoor, who provided the pCMV NS5 expression plasmid, which was constructed during graduate studies in Dr. Padmanabhan's laboratory at the University of Kansas Medical Center (Kansas City, KS).

REFERENCES

1. Guzman, M. G., Halstead, S. B., Artsob, H., Buchy, P., Farrar, J., Gubler, D. J., Hunsperger, E., Kroeger, A., Margolis, H. S., Martínez, E., Nathan, M. B., Pelegrino, J. L., Simmons, C., Yoksan, S., and Peeling, R. W. (2010) Dengue: a continuing global threat. *Nat. Rev. Microbiol.* **8,** S7–S16
2. Mitka, M. (2013) Dengue more prevalent than previously thought. *JAMA* **309,** 1882
3. Halstead, S. B. (2007) Dengue. *Lancet* **370,** 1644–1652
4. Egloff, M. P., Benarroch, D., Selisko, B., Romette, J. L., and Canard, B. (2002) An RNA cap (nucleoside-2′-*O*-)-methyltransferase in the flavivirus RNA polymerase NS5: crystal structure and functional characterization. *EMBO J.* **21,** 2757–2768
5. Ray, D., Shah, A., Tilgner, M., Guo, Y., Zhao, Y., Dong, H., Deas, T. S., Zhou, Y., Li, H., and Shi, P. Y. (2006) West Nile virus 5′-cap structure is formed by sequential guanine N-7 and ribose 2′-*O* methylations by nonstructural protein 5. *J. Virol.* **80,** 8362–8370
6. Egloff, M. P., Decroly, E., Malet, H., Selisko, B., Benarroch, D., Ferron, F., and Canard, B. (2007) Structural and functional analysis of methylation and 5′-RNA sequence requirements of short capped RNAs by the methyltransferase domain of dengue virus NS5. *J. Mol. Biol.* **372,** 723–736
7. Dong, H., Ray, D., Ren, S., Zhang, B., Puig-Basagoiti, F., Takagi, Y., Ho, C. K., Li, H., and Shi, P. Y. (2007) Distinct RNA elements confer specificity to flavivirus RNA cap methylation events. *J. Virol.* **81,** 4412–4421
8. Zhou, Y., Ray, D., Zhao, Y., Dong, H., Ren, S., Li, Z., Guo, Y., Bernard, K. A., Shi, P. Y., and Li, H. (2007) Structure and function of flavivirus NS5 methyltransferase. *J. Virol.* **81,** 3891–3903
9. Liu, L., Dong, H., Chen, H., Zhang, J., Ling, H., Li, Z., Shi, P. Y., and Li, H. (2010) Flavivirus RNA cap methyltransferase: structure, function, and inhibition. *Front. Biol.* **5,** 286–303
10. Dong, H., Chang, D. C., Hua, M. H., Lim, S. P., Chionh, Y. H., Hia, F., Lee, Y. H., Kukkaro, P., Lok, S. M., Dedon, P. C., and Shi, P. Y. (2012) 2′-*O* methylation of internal adenosine by flavivirus NS5 methyltransferase. *PLoS Pathog.* **8,** e1002642
11. Bartelma, G., and Padmanabhan, R. (2002) Expression, purification, and characterization of the RNA 5′-triphosphatase activity of dengue virus type 2 nonstructural protein 3. *Virology* **299,** 122–132
12. Benarroch, D., Selisko, B., Locatelli, G. A., Maga, G., Romette, J. L., and Canard, B. (2004) The RNA helicase, nucleotide 5′-triphosphatase, and RNA 5′-triphosphatase activities of dengue virus protein NS3 are Mg^{2+}-dependent and require a functional Walker B motif in the helicase catalytic core. *Virology* **328,** 208–218
13. Issur, M., Geiss, B. J., Bougie, I., Picard-Jean, F., Despins, S., Mayette, J., Hobdey, S. E., and Bisaillon, M. (2009) The flavivirus NS5 protein is a true RNA guanylyltransferase that catalyzes a two-step reaction to form the RNA cap structure. *RNA* **15,** 2340–2350
14. Decroly, E., Ferron, F., Lescar, J., and Canard, B. (2012) Conventional and unconventional mechanisms for capping viral mRNA. *Nat. Rev. Microbiol.* **10,** 51–65
15. Xagorari, A., and Chlichlia, K. (2008) Toll-like receptors and viruses: induction of innate antiviral immune responses. *Open Microbiol. J.* **2,** 49–59
16. Tan, B. H., Fu, J., Sugrue, R. J., Yap, E. H., Chan, Y. C., and Tan, Y. H. (1996) Recombinant dengue type 1 virus NS5 protein expressed in *Escherichia coli* exhibits RNA-dependent RNA polymerase activity. *Virology* **216,** 317–325
17. Ackermann, M., and Padmanabhan, R. (2001) *De novo* synthesis of RNA by the dengue virus RNA-dependent RNA polymerase exhibits temperature dependence at the initiation but not elongation phase. *J. Biol. Chem.* **276,** 39926–39937
18. Nomaguchi, M., Ackermann, M., Yon, C., You, S., and Padmanabhan, R. (2003) *De* novo synthesis of negative-strand RNA by dengue virus RNA-dependent RNA polymerase in vitro: nucleotide, primer, and template parameters. *J. Virol.* **77,** 8831–8842
19. Kapoor, M., Zhang, L., Ramachandra, M., Kusukawa, J., Ebner, K. E., and Padmanabhan, R. (1995) Association between NS3 and NS5 proteins of dengue virus type 2 in the putative RNA replicase is linked to differential phosphorylation of NS5. *J. Biol. Chem.* **270,** 19100–19106
20. Mackenzie, J. M., Khromykh, A. A., Jones, M. K., and Westaway, E. G. (1998) Subcellular localization and some biochemical properties of the flavivirus Kunjin nonstructural proteins NS2A and NS4A. *Virology* **245,** 203–215
21. Westaway, E. G., Mackenzie, J. M., and Khromykh, A. A. (2003) Kunjin RNA replication and applications of Kunjin replicons. *Adv. Virus Res.* **59,** 99–140
22. Lindenbach, D., Thiel, H. J., and Rice, C. (2007) in *Field's Virology*, 5th Ed. (Knipe, D. M., and Howley, P. M., eds) pp. 1101–1152, Lippincott-Raven Publishers, Philadelphia
23. Bartenschlager, R., and Miller, S. (2008) Molecular aspects of Dengue virus replication. *Future Microbiol.* **3,** 155–165
24. Padmanabhan, R., and Strongin, A. Y. (2010) in *Frontiers in Dengue Virus Research* (Hanley, K. A., and Weaver, S. C., eds) pp 14–33, Caister Academic Press, Norfolk, UK
25. Gebhard, L. G., Kaufman, S. B., and Gamarnik, A. V. (2012) Novel ATP-independent RNA annealing activity of the dengue virus NS3 helicase. *PloS One* **7,** e36244
26. Yon, C., Teramoto, T., Mueller, N., Phelan, J., Ganesh, V. K., Murthy, K. H., and Padmanabhan, R. (2005) Modulation of the nucleoside triphosphatase/RNA helicase and 5′-RNA triphosphatase activities of dengue virus type 2 nonstructural protein 3 (NS3) by interaction with NS5, the RNA-dependent RNA polymerase. *J. Biol. Chem.* **280,** 27412–27419
27. Luo, D., Wei, N., Doan, D. N., Paradkar, P. N., Chong, Y., Davidson, A. D., Kotaka, M., Lescar, J., and Vasudevan, S. G. (2010) Flexibility between the protease and helicase domains of the dengue virus NS3 protein conferred by the linker region and its functional implications. *J. Biol. Chem.* **285,** 18817–18827
28. Polo, S., Ketner, G., Levis, R., and Falgout, B. (1997) Infectious RNA transcripts from full-length dengue virus type 2 cDNA clones made in yeast. *J. Virol.* **71,** 5366–5374
29. Teramoto, T., Kohno, Y., Mattoo, P., Markoff, L., Falgout, B., and Padmanabhan, R. (2008) Genome 3′-end repair in dengue virus type 2. *RNA* **14,** 2645–2656
30. Spencer, F., Ketner, G., Connelly, C., and Hieter, P. (1993) Targeted recombination-based cloning and manipulation of large DNA segments in yeast. *Methods* **5,** 161–175
31. Zeng, L., Falgout, B., and Markoff, L. (1998) Identification of specific nucleotide sequences within the conserved 3′-SL in the dengue type 2 virus genome required for replication. *J. Virol.* **72,** 7510–7522
32. Manzano, M., Reichert, E. D., Polo, S., Falgout, B., Kasprzak, W., Shapiro, B. A., and Padmanabhan, R. (2011) Identification of cis-acting elements in the 3′-untranslated region of the dengue virus type 2 RNA that modulate translation and replication. *J. Biol. Chem.* **286,** 22521–22534
33. You, S., and Padmanabhan, R. (1999) A novel *in vitro* replication system for dengue virus. Initiation of RNA synthesis at the 3′-end of exogenous viral RNA templates requires 5′- and 3′-terminal complementary sequence motifs of the viral RNA. *J. Biol. Chem.* **274,** 33714–33722
34. Boonyasuppayakorn, S., and Padmanabhan, R. (2014) Construction of plasmid, bacterial expression, purification, and assay of Dengue virus type 2 NS5 methyltransferase. *Methods Mol. Biol.* **1138,** 361–373
35. Kapoor, M. (1995) *Construction of an Infectious Clone for Dengue Virus Type 2 and Characterization of the Putative Viral RNA-dependent RNA Polymerase*, Ph.D. thesis, University of Kansas Medical Center, Kansas City, KS
36. Navarro-Sánchez, E., Desprès, P., and Cedillo-Barrón, L. (2005) Innate immune responses to dengue virus. *Arch. Med. Res.* **36,** 425–435
37. Morrison, J., Aguirre, S., and Fernandez-Sesma, A. (2012) Innate immunity evasion by dengue virus. *Viruses* **4,** 397–413
38. You, S., Falgout, B., Markoff, L., and Padmanabhan, R. (2001) *In vitro* RNA synthesis from exogenous dengue viral RNA templates requires long range interactions between 5′- and 3′-terminal regions that influence RNA structure. *J. Biol. Chem.* **276,** 15581–15591
39. Yu, L., Nomaguchi, M., Padmanabhan, R., and Markoff, L. (2008) Specific requirements for elements of the 5′ and 3′ terminal regions in flavivirus RNA synthesis and viral replication. *Virology* **374,** 170–185
40. Arroyo, J., Miller, C. A., Catalan, J., and Monath, T. P. (2001) Yellow fever vector live-virus vaccines: West Nile virus vaccine development. *Trends Mol. Med.* **7,** 350–354

41. Durbin, A. P., McArthur, J. H., Marron, J. A., Blaney, J. E., Thumar, B., Wanionek, K., Murphy, B. R., and Whitehead, S. S. (2006) rDEN2/4Delta30(ME), a live attenuated chimeric dengue serotype 2 vaccine is safe and highly immunogenic in healthy dengue-naive adults. *Hum. Vaccin.* **2,** 255–260
42. Blaney, J. E., Jr., Sathe, N. S., Goddard, L., Hanson, C. T., Romero, T. A., Hanley, K. A., Murphy, B. R., and Whitehead, S. S. (2008) Dengue virus type 3 vaccine candidates generated by introduction of deletions in the 3′ untranslated region (3′-UTR) or by exchange of the DENV-3 3′-UTR with that of DENV-4. *Vaccine* **26,** 817–828
43. Khromykh, A. A., and Westaway, E. G. (1997) Subgenomic replicons of the flavivirus Kunjin: construction and applications. *J. Virol.* **71,** 1497–1505
44. Khromykh, A. A., Meka, H., Guyatt, K. J., and Westaway, E. G. (2001) Essential role of cyclization sequences in flavivirus RNA replication. *J. Virol.* **75,** 6719–6728
45. Kümmerer, B. M., and Rice, C. M. (2002) Mutations in the yellow fever virus nonstructural protein NS2A selectively block production of infectious particles. *J. Virol.* **76,** 4773–4784
46. Dong, H., Chang, D. C., Xie, X., Toh, Y. X., Chung, K. Y., Zou, G., Lescar, J., Lim, S. P., and Shi, P. Y. (2010) Biochemical and genetic characterization of dengue virus methyltransferase. *Virology* **405,** 568–578
47. Khromykh, A. A., Kenney, M. T., and Westaway, E. G. (1998) *trans*-Complementation of flavivirus RNA polymerase gene NS5 by using Kunjin virus replicon-expressing BHK cells. *J. Virol.* **72,** 7270–7279
48. Noble, C. G., and Shi, P. Y. (2012) Structural biology of dengue virus enzymes: towards rational design of therapeutics. *Antiviral Res.* **96,** 115–126
49. Kroschewski, H., Lim, S. P., Butcher, R. E., Yap, T. L., Lescar, J., Wright, P. J., Vasudevan, S. G., and Davidson, A. D. (2008) Mutagenesis of the dengue virus type 2 NS5 methyltransferase domain. *J. Biol. Chem.* **283,** 19410–19421
50. Lu, G., and Gong, P. (2013) Crystal Structure of the full-length Japanese encephalitis virus NS5 reveals a conserved methyltransferase-polymerase interface. *PLoS Pathog.* **9,** e1003549
51. Vasudevan, S. G., Johansson, M., Brooks, A. J., Llewellyn, L. E., and Jans, D. A. (2001) Characterisation of inter- and intra-molecular interactions of the dengue virus RNA dependent RNA polymerase as potential drug targets. *Farmaco* **56,** 33–36
52. Johansson, M., Brooks, A. J., Jans, D. A., and Vasudevan, S. G. (2001) A small region of the dengue virus-encoded RNA-dependent RNA polymerase, NS5, confers interaction with both the nuclear transport receptor importin-β and the viral helicase, NS3. *J. Gen. Virol.* **82,** 735–745
53. Zou, G., Chen, Y. L., Dong, H., Lim, C. C., Yap, L. J., Yau, Y. H., Shochat, S. G., Lescar, J., and Shi, P. Y. (2011) Functional analysis of two cavities in flavivirus NS5 polymerase. *J. Biol. Chem.* **286,** 14362–14372
54. Takahashi, H., Takahashi, C., Moreland, N. J., Chang, Y. T., Sawasaki, T., Ryo, A., Vasudevan, S. G., Suzuki, Y., and Yamamoto, N. (2012) Establishment of a robust dengue virus NS3-NS5 binding assay for identification of protein-protein interaction inhibitors. *Antiviral Res.* **96,** 305–314
55. Vignuzzi, M., Stone, J. K., Arnold, J. J., Cameron, C. E., and Andino, R. (2006) Quasispecies diversity determines pathogenesis through cooperative interactions in a viral population. *Nature* **439,** 344–348